CHAPTER 3

MATERIALS AND METHODS

3.1 CHEMICALS AND REAGENTS

All chemicals used were of analytical grade, and were purchased from Merck (South Africa), unless stated otherwise. All gases of highest purity standard were purchased from African Oxygen Limited (Afrox) (South Africa). Sr, Co and Cs stock solutions were prepared by dissolving 3.0429g of $SrCl_2.6H_2O$, 4.9383g of $Co(NO_3)_2.6H_2O$ and 1.267g CsCl, respectively, in 10mL HNO_3/distilled water solution (1:1) and then diluted to 1 L to give a final concentration of 1000 mg/L of each metal. Working concentrations and standard solutions were prepared by diluting the stock solution with distilled water to give the desired concentration. All glassware was soaked in 10% HNO_3 and rinsed with distilled water prior to and after use.

3.2 MICROORGANISM

A mixed sulphate reducing bacteria (SRB) starter culture previously isolated from a coal mine waste site was kindly supplied by Dr. Harma Greben (CSIR, Pretoria, South Africa). In previous studies, a range of radionuclides, have been shown to be present in coal samples. In addition, low to high radioactivity levels have also been detected around coal mines (Jamil et al., 1998; Jasinska et al., 1998). Therefore, the use of the present SRB cultures for Sr, Co and Cs uptake experiments was based on the hypothesis that the cultures are acclimatized to high metal and radionuclide concentrations. Initial kinetic sorption performance parameters for Sr, Co and Cs removal by growing SRB cultures were determined in batch anaerobic bioreactors (2L) incubated at 25±0.5°C with continuous stirring at 120 rpm. Further batch experiments were conducted in 100 mL serum bottles to evaluate the kinetic and equilibrium sorption parameters of the SRB cultures under non-growth conditions.

3.3 MEDIA

SRB enrichments were performed according to a procedure by Butlin et al. (1949) using medium B, a liquid medium containing sulphate, lactate and a trace of ferrous salt (Table 3.1). The media was sterilized using a Tomin TM-323 autoclave (Durawell Co. Limited, Taiwan). The microorganisms were incubated in the dark at 30±2°C with continuous stirring at 120 rpm. The anaerobic growth vessel was regularly flushed with 99.9% N_2 gas to maintain an anaerobic atmosphere. When considerable blackening of the medium had occurred (due to FeS formation), which took up to 28 days, the culture was examined to determine cell concentration using the total bacteria count (TBC) method. The enrichment procedure was repeated until the desired viable cell concentration was obtained. A 10 L stock culture bioreactor was started by aseptically transferring a 10% (v/v) of the enriched cultures into medium C. The stock culture was sub-cultured every 3-4 weeks by transferring the culture to freshly prepared medium C. This medium was selected on the basis of its lack of iron, as blackening of growth medium interferes with analytical procedures for metal biosorption experiments.

Table 3.1 Composition of media for SRB enrichment and growth.

Component	Composition per litre	
	Medium B	Medium C
Sodium lactate (60 % solution)	5 mL	6 mL
$MgSO_4.7H_2O$	2.0g	0.1 g
Na_2SO_4	-	4.5 g
NH_4Cl	1.0g	1.0 g
$CaSO_4$	1.0g	-
$CaCl_2.6H_2O$	-	0.06g
$FeSO_4.(NH_4)_2SO_4.6H_2O$	0.5g	-
Yeast extract	1.0 g	1.0 g
K_2HPO_4	0.5 g	-
KH_2PO_4	-	0.5g
$Na_2SO_3.7H_2O$	0.03g	-
Ascorbic acid	-	0.1 g
Sodium thioglycollate	-	0.1 g
Sodium citrate.$2H_2O$	-	0.1 g

3.4 BATCH SRB BIOREACTOR EXPERIMENTS

3.4.1 Bioreactor Configuration

The batch SRB bioreactor used for preliminary kinetic metal sorption experiments was a closed anaerobic system, which was constructed from a 2L Pyrex glass Erlenmeyer flask (Figure 3.1). Prior to bioreactor system assembly, the reaction vessel (bioreactor) was filled with 1.5 L medium C spiked with the target metal, and autoclaved together with the magnetic stirrer bar. The bioreactor was then immediately sealed with an airtight rubber stopper, and purged with high purity (99.9%) nitrogen gas to maintain anaerobic conditions. A 10% (w/v) zinc acetate solution was connected to reaction vessel to trap the hydrogen sulphide gas produced in the bioreactor. Samples were withdrawn using a sterile hypodermic syringe attached to a glass tube. Bioreactor mixing was achieved by means of an AM4 multiple heating magnetic stirrer (Velp Scientifica, Labex Pty Ltd, South Africa) in conjunction with stirrer bars.

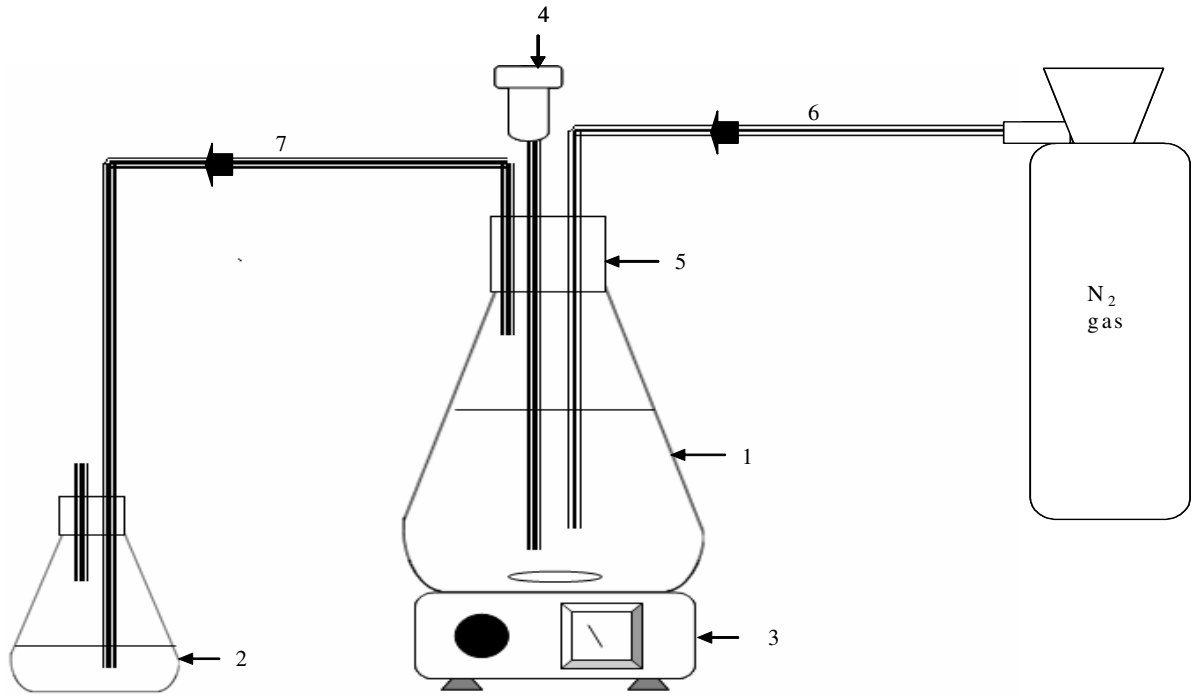

Figure 3.1: Schematic diagram of the laboratory-scale anaerobic SRB batch bioreactor. (1= anaerobic bioreactor, 2= 10% zinc acetate trap solution, 3= magnetic stirrer, 4= sampling syringe, 5= rubber stopper, 6= N_2 gas inlet and 7= H_2S gas outlet).

3.4.2 SRB Screening for Sr, Co and Cs Removal and Tolerance

Preliminary studies aimed at screening for selective Sr, Co and Cs removal and tolerance among individual cultures in the bacterial consortium were performed in a series of batch SRB bioreactors. Each of the batch bioreactors filled with growth medium supplemented with each metal at an initial concentration of 75 mg/L, were inoculated with a 5 mL culture sample containing 1.6×10^8 cells/mL of viable mixed SRB cells. All experiments were conducted in duplicate. The suspensions were incubated under optimal SRB growth conditions for up to 28 days. At the end of the incubation period, samples were removed for monitoring changes in the phylogeny of the original SRB as a result of exposure to the different metals. Prior to culture isolation in agar plates, enrichments for each sample were prepared as described before. SRB growth medium without metal but the bacterial inoculum (bacterial growth control) and medium with metal but without bacterial inoculum (abiotic control) served as controls.

3.4.3 Kinetics of Sr^{2+}, Co^{2+} and Cs^{+} Removal in the SRB Bioreactor

The removal of different initial Sr^{2+}, Co^{2+} and Cs^{+} concentrations (25-500 mg/L) and their effect on the growth and metabolism of the SRB consortium was also investigated. The suspensions were incubated under optimal SRB growth conditions for up to 14 days. Sampling was carried out daily over the entire incubation period, for sulphate, sulphide, residual metal concentration, pH analysis, as well as total biomass count. Prior to analysis, the samples were clarified by means of a Hermle Z 323 centrifuge (Memingen, Germany). Subsequent to centrifugation, the microbial component of bacterial suspensions was separated using a 0.22µm (Millipore, USA) filter paper. Results obtained were compared to with those from control experiments, consisting of bioreactors inoculated with viable SRB cells in the absence of Sr, Co and Cs, and bioreactors containing medium with metal but without bacterial inoculum (abiotic control). To determine the nature of the mechanism of Sr^{2+}, Cs^{+} and Co^{2+} removal from solution, metal-loaded SRB cells were subjected to a five-step desorption procedure (Tessier et al., 1979). Obtained results were compared with those obtained for Sr, Co and Cs removal by dead SRB cells (killed by autoclaving at 121ºC and 15 psi for 20 minutes).

3.4.4 Model Formulations for SRB Bioreactor Processes

The reaction schemes, rate equations and kinetic constants used for the biological processes; biomass population dynamics and sulphate reduction were adapted from literature. Different models have been proposed to describe the growth kinetics of a microbial population growing with a single limiting substrate. However, a study by Senn et al. (1994) has shown that out of several proposed, the Monod model (Monod, 1949) has been used extensively as the model parameters μ, μ_{max}, S and K_s have a biological meaning and are experimentally accessible. The Monod model describes the relationship between μ the specific growth rate) and S (substrate concentration) by a type of saturation kinetics as shown in Equation 3.1.

$$\mu = \mu_{\max} \frac{S}{K_s + S} \qquad [3.1]$$

Where: μ is the specific growth rate (1/h), μ_{max} the maximum specific growth rate (1/h), S the substrate concentration (mg/L) and K_s is the substrate affinity, i.e. the substrate concentration at which the cells grow at half maximum specific growth rate (mg/L).

To account for bacterial population growth, in the presence of a metal (inhibitor), a simple Monod's non-competitive inhibition kinetic model, incorporating an inhibition term, I, in which K_i is the inhibition coefficient, was used to model bacteria growth (Equation 3.2). Parameters for biological sulphate reduction in the presence of Sr^{2+}, Co^{2+} and Cs^{+} were estimated using the Pirt equation (Equation 3.3) as previously done by Kalyuzhnyi et al. (1998), and Robinson and Tiedje (1983). The sulphate concentration levels were assumed to be non inhibitory. Inhibition due to sulphide formation was assumed not significant as the sulphide concentration in the batch system at any time was much lower than the reported inhibition concentration (300–550 mg/L of sulphide is necessary to impart sulphide inhibition). The reactor was assumed to be completely mixed, and pH was kept constant in a narrow range (pH 6.8–7.2, unless stated otherwise). Thus, there was no inhibition associated acidic or alkaline conditions in the reactors. A second-order rate equation (Equation 3.5), based on the solute concentration, and incorporating an active biomass term was used to predict metal (Sr^{2+}, Co^{2+} and Cs^{+}) removal over time in the bioreactors.

$$\frac{dX}{dt} = \left(\frac{\mu_{\max} SX}{K_s + S} \right) \times I \qquad [3.2]$$

$$-\frac{dS}{dt} = \frac{1}{Y_{x/s}} \left(\frac{dX}{dt} \right) \qquad [3.3]$$

$$I = \frac{Ki}{Ki + C} \qquad [3.4]$$

$$-\frac{dC}{dt} = k_C CX \qquad [3.5]$$

where; μ_{max} is the maximum specific growth rate coefficient (1/h), K_s is the half saturation constant (mg/L), S is the concentration of substrate at time t (mg/L), $Y_{x/s}$ is the bacterial yield coefficient (mg of biomass produced per mg substrate utilized), X is the concentration of biomass at time t (mg/L), k_C is the second-order rate coefficient (L/mg/h) and C is the metal concentration at time t (mg/L).

3.4.5 Modelling Software

In this study, the computer program AQUASIM 2.0 (Reichert, 1998) was used for all bioreactor processes modeling. AQUASIM is a computer program for the identification and simulation of aquatic systems. The program can be used to calculate substrate removal in bioreactors for any user specified microbial system. AQUASIM extends the capabilities of conventional environmental simulation programs mainly in. two ways: (1) the program does not implement a specific model, but allow users to specify models as freely as possible and (2) it offers system identification tasks in addition to simulation. AQUASIM performs simulations by comparing calculated results with measured data, and such simulations are then used to validate model assumptions. Systematic deviations between calculated and measured values may suggest that additional important processes are to be considered or corrections are needed in the formulation

of processes. Another important functionality of AQUASIM is automatic parameter estimation for a given model structure using measured data. These estimations are done using the weighted least-squares technique. This is not only important for getting neutral estimates of parameters, but it is a prerequisite for efficiently comparing different models. Several calculations with several target variables, and universal as well as calculation-specific parameters, can be combined to a single parameter estimation process. This is a very important feature not present in most of the statistical software. This software has been successfully used by a number of researchers to describe SRB bioreactor processes (Kosseva and Hansford, 2001; Ristow and Hansford, 2001). The program AQUASIM estimated the best fit by minimizing the χ^2 values as shown in Equation 3.6. However, the goodness of fit χ^2 values may be subject to bias due to multivariate non-normality. If data from the model are similar to the experimental data, χ^2 will be a small number; if they are different, χ^2 will be a large number. For each metal set, the sensitivity of the kinetic parameters related to the SRB bioreactor processes; biomass, substrate and metal concentrations, was also computed using AQUASIM 2.0.

$$\chi^2 = \Sigma \frac{\left(S_{exp} - S_{mod}\right)^2}{S_{mod}} \qquad [3.6]$$

where: $S_{,mod}$ is the calculated (model) concentration at time t (mg/L), and $S_{,exp}$ is the experimental concentration at time t (mg/L).

3.5 KINETICS OF Sr^{2+}, Co^{2+} and Cs^{+} BIOSORPTION FROM AQUEOUS SOLUTION

3.5.1 Kinetic experiments

Kinetic sorption experiments for the effect of initial concentration, biomass concentration, metabolic state and pH on the removal of Sr^{2+}, Co^{2+} and Cs^{+} from single metal aqueous solutions were performed in 100 mL rubber-sealed serum bottles. The bacterial consortium used for the metal biosorption studies was reconstituted by combining all the bacterial isolates detected in both non-contaminated and contaminated bioreactors. The initial metal concentration and pH were varied between 25-500 mg/L and 2-9, respectively, and the biomass cell density was kept constant at 0.5 g/L. For the biomass concentration studies, cell density was varied between 0.5-3 g/L, while the initial metal concentration and pH were kept constant at 75 mg/L and 4,

respectively. To determine the effect of bacterial metabolic state, live and heat-killed bacteria cells were exposed to the different metals at an initial concentration of 75 mg/L and pH 4. SRB cells suspended in aqueous solution but without metal and aqueous metal solution but without bacterial inoculum (abiotic control) served as controls. In all experiments, samples (1 mL) were removed at timed intervals by sterile syringes for residual metal analysis. Metal concentration was determined by the AAS. The metal uptake capacity (q_{eq}) was calculated as:

$$q_{eq} = \frac{(C_{ini} - C_{eq})}{X} \qquad [3.7]$$

where: q_{eq} = metal uptake capacity (mg/g), C_{ini} = initial concentration of metal in solution (mg/L), C_{eq} = equilibrium concentration of metal in solution (mg/L), and X = dry weight of SRB added (g).

3.5.2 Kinetic Modelling

In an attempt to clarify the mechanism of Sr^{2+}, Co^{2+} and Cs^{+} removal from aqueous solution by SRB cells, and identify the main factors controlling sorption rate such as; mass transport, pore diffusion and chemical reaction processes, the first-order (Lagergren, 1898), pseudo-second-order (Ho and McKay, 1999), and external and intraparticle diffusion (Weber and Morris, 1963) kinetic models were evaluated.

The linearised pseudo-first and second order models can be expressed as follows:

$$\ln(q_{eq} - q_t) = \ln q_{eq} - k_1 t \qquad [3.8]$$

$$\frac{t}{q_t} = \frac{1}{k_2 q_{eq}^2} + \frac{t}{q_{eq}} \qquad [3.9]$$

where: q_t = concentration of ion species in the sorbent at time t (mg/g), q_{eq} = equilibrium concentration of adsorbed ionic species in the sorbent (mg/g), k_1= biosorption constant of pseudo-first-order Lagergren equation (min^{-1}) and k_2 = biosorption constant of pseudo-second-order Lagergren equation (min/ g/mg). The applicability of the pseudo-first and second order

models was determined by linear regression method, from which sorption parameters were determined.

For a solid-liquid sorption process, the solute transfer is usually characterized by either external mass transfer (boundary layer diffusion) or intraparticle diffusion or both. If external diffusion of metal cations (within the diffuse layers outside the sorbent) is the rate-limiting step then it has been shown that Equation 3.11 can be fitted into sorption data with some success.

$$\ln\frac{C_t}{C_{ini}} = -\mathrm{k_f}\frac{A}{V}\mathrm{t} \qquad [3.11]$$

where: C_{ini} = initial metal concentration (mg/L), C_t = metal concentration at time t (mg/L), A=external sorption area (m^2/g), V= total solution volume (L), and k_f = the external diffusion coefficient (cm/s). However, when intraparticle diffusion (transfer of metal cations from the adsorbent surface to the internal active binding sites) is the rate-limiting step, then sorption data can be described by Equation 3.12, as proposed by Weber and Morris in 1962;

$$q_t = k_i t^{0.5} \qquad [3.12]$$

where: q_t = concentration of ion species in the sorbent at time t (mg/g) and k_i = the intraparticle diffusion rate (mg.g.$min^{0.5}$).

The applicability of the external and intraparticle diffusion model was determined by linear regression method, from which sorption parameters were determined. For the external diffusion model, if the experimental data (a plot of $\ln(C_t/C_{ini})$ against time t), conforms to a linear plot with a high correlation coefficient (R^2), then external diffusion is the rate-limiting step. The external diffusion coefficient k_f (cm/s) can be calculated from the slope of the straight line obtained from Equation 3.10. On the other hand, if a plot of the experimental data (q_t against $t^{0.5}$) conforms to a linear plot and the line passes through origin, then intraparticle diffusion is the rate-limiting step (Webber and Morris, 1963). The intraparticle diffusion rate coefficient is given by the slope of the line.

3.6 MAXIMUM BIOSORPTION CAPACITY OF Sr^{2+}, Co^{2+} AND Cs^{+}

3.6.1 Equilibrium Sorption Experiments

Batch equilibrium sorption experiments were carried out using standard batch methodology as described by Volesky (1990). The equilibrium removal of Sr^{2+}, Co^{2+} and Cs^{+} from single and binary metal solutions was evaluated. For these studies, the bacterial consortium used was reconstituted combination of all the bacterial isolates detected in both non-contaminated and contaminated bioreactors. The initial concentration was varied between 25 and 1200 mg/L for single metal isotherms. The competitive removal of metal ions from binary metal solutions was carried out by adding equivalent initial concentrations of the target and competing metal ion ranging from 25 to 1200 mg/L. In all experiments, pH and SRB cell density were kept constant at 4 and 0.5 g/L, respectively. SRB cells suspended in aqueous solution metal but without metal and aqueous metal solution but without bacterial inoculum (abiotic control) served as controls. Samples (1mL) were removed by sterile syringes at equilibrium for residual metal analysis. Metal concentration was determined by the AAS.

3.6.2 Equilibrium isotherm modeling

The applicability of well established empirical models, such as the classical Langmuir (Langmuir, 1918) and Freundlich (Freundlich, 1907) equilibrium sorption isotherms in the present sorption process are evaluated. The Langmuir equation can be expressed as:

$$q = \frac{q_{max}\, bC_{eq}}{1 + bC_{eq}} \qquad [3.13]$$

This models incorporates two constants that are easy to interpret; q_{max}, the maximum sorbate uptake (mg/g), and *b,* the coefficient related to the affinity between the sorbent and sorbate. q = sorption uptake (mg/g). On the hand, the Freundlich equation can be expressed as:

$$q = kC_{eq}^{(1/n)} \qquad [3.14]$$

This model also incorporates two constants: k, which corresponds to the binding capacity; and n, which characterises the affinity between the bacterial sorbent and metal. C_{eq} = equilibrium concentration of the sorbate remaining in the solution (mg/L). In order to verify the good compliance of the experimental data to the empirical (Langmuir and Freundlich isotherms) models, a non linear regression method was used to construct model curves, from which equilibrium parameters were estimated.

3.7 ADSORPTION OF PROTONS AND Sr^{2+}, Co^{2+} AND Cs^{+} ONTO SRB CELLS

3.7.1 Preparation of Bacterial Adsorbent

A mixed SRB bacteria culture was obtained by combining all the bacterial isolates detected in both non-contaminated and contaminated bioreactors. The microorganisms were grown in stock in Postgate medium C for about 5-7 days, after which the actively growing bacteria cells were harvested and aseptically transferred to 2L rubber-sealed batch anaerobic bioreactors and allowed to grow in fresh Postgate Medium C. The cells were allowed to grow until mid-stationary phase (5-7 days). Equal volumes of liquid bacteria culture were dispensed into centrifuge tubes, and the bacteria were harvested from the growth media by centrifugation (6000 ×g, 15 minutes). Cells were repeatedly washed in deionized water to remove growth medium impurities. Metal cations that maybe present on SRB cell wall surfaces were stripped by soaking in 0.001M EDTA for 30 minutes, followed by intensive rinsing in deionized water. Finally cells were then subjected to two final rinses in a $NaNO_3$ electrolyte solution without an acid wash step to prevent any damage to the outer membrane of the gram negative species. The ionic strength of the electrolyte wash solution was varied according to that of the experiment in which the bacteria were to be used.

3.7.2 Metal Adsorption Experiments

Experiments for Sr, Cs and Co adsorption onto SRB cells were conducted under anaerobic conditions as a function of pH, ionic strength and temperature. Prior to use, the bottles were cleaned by soaking in two successive acid baths (10% v/v HNO_3) for 24 hours each, rinsed twice in ultra-pure water, and then dried in an oven at 105ºC. For each metal, a stock bacterial suspension consisting of a known mass of bacteria suspended in an electrolyte solution (0.1 M $NaNO_3$ or unless otherwise stated) was prepared. The stock bacterial suspension was then

supplemented with the target metal obtained from 1000 mg/L metal stock solution (prepared in 0.1 M $NaNO_3$) to yield the required initial concentration. The initial concentrations for Sr, Cs and Co were chosen based on calculations using MINTEQA2 (Allison et al., 1991) to circumvent premature metal precipitation with increasing pH. After the addition of the metal, the pH of the bacterial-metal stock suspension was recorded. The suspension was then divided into a series of 100 mL serum bottles, and the pH was adjusted to the desired value by adding small volumes of concentrated HNO_3 or NaOH solution. In all the experiments, the pH was allowed to drift, and the final pH of the suspension was recorded at the end of the equilibration period. After pH adjustment, the serum bottles were immediately sealed with airtight rubber stoppers, and incubated in a Labcon SPL-MP 15 Orbital Shaker (Labcon Laboratory Services, South Africa) at 100 rpm, and allowed to equilibrate for 3 hours at 25±0.5°C. All experiments were performed repeatedly in triplicates. At the end of the equilibration period samples were collected by sterile syringes equipped with a needle, which was inserted into the rubber stoppers. The collected sample was clarified by centrifugation. The clear supernatant was acidified to 1% v/v HNO_3 and stored at 4 °C before metal analysis.

3.7.3 Surface Complexation Modeling

In this study, FITMOD, a modified version of the computer program FITEQL 2.0 (Westall, 1982) was used to construct geochemical models describing proton interaction with the bacteria (Daughney et al., 2004). FITMOD incorporates a number of models; both nonelectrostatic and electrostatic double layer models. This program utilizes the proton balance approach to optimize protonation constants of the various functional groups on the bacterial surface. SRB titration experimental data obtained was plotted in terms of the concentration of deprotonated or protonated sites per mass of SRB (mol/g), using Equation 3.15.

$$[H^+]_{\text{added/released}} = (C_a - C_b - [H^+] + [OH^-])/m_b \qquad [3.15]$$

where: C_a, C_b, $[H^+]$ and $[OH^-]$ are the molar concentrations of acid, base, H^+ and OH^- species, respectively, and m_b is the weight of SRB cells (mg/L) in the suspension.

The mass law relationship in conjunction with the mole balance expressions was used to define the adsorptive process. A 1:1 metal/surface site stoichometry was used for all calculations, and equilibrium constants for aqueous metal hydrolysis were obtained from Baes and Mesmer (1979). This information was used to account for Sr, Co and Cs adsorption onto SRB cell surfaces according to Equation 3.16. Under equilibrium conditions partitioning between the solid surface and the aqueous phase is therefore quantified with the corresponding mass law (Equation 3.17).

$$M^{+} + R - A^{-} \Leftrightarrow R - AM \qquad [3.16]$$

$$K_{ads} = \frac{[R - AM]}{[M^{+}] \times [R - A^{-}]} \qquad [3.17]$$

where: M^{+} = target metal, R-A^{-} = deprotonated bacterial surface site, R-AM = metal-site complex, K_{ads} = thermodynamic equilibrium constant for the reaction, and brackets denote concentrations of the specified species.

The goodness-of-fit of the different models to the titration data is indicated by the overall variance, V(Y), which is calculated by FITMOD as shown in Equation 3.18. Values of V(Y) between 1 and 20 generally indicate an acceptable fit to the data (Daughney et al., 2004).

$$V(Y) = \frac{Y_{II}^{P\left(\frac{Y}{S_Y}\right)^2}}{n_p \bullet n_{II} - n_u} \qquad [3.18]$$

where: Y is the error in the mass balance calculations, S_Y is the default experimental error calculated by FITMOD, n_p is the number of data points, n_{II} is the number of chemical components for which both total and free concentrations are known, and n_u is the number of adjustable parameters.

3.8 ANALYTICAL PROCEDURES

3.8.1 Bacterial Culture Characterization

Gram Staining

Gram staining of SRB was carried out as described by Shimeld and Rodgers (1999). At mid-stationary phase, a 0.5 mL sample of sulphate reducing bacteria culture was aseptically withdrawn with a sterile syringe. The sample was smeared on a slide, soaked in a violet dye and then treated with iodine. The slide was then rinsed with alcohol and counterstained with safranine. The result was viewed on a phase microscope.

Phylogenetic Analysis

Culture isolation was carried out using a method by Butlin et al. (1949) in medium A, solidified by 2.3% agar. An aliquot of 9 mL of cooled liquid agar medium was mixed with 1 mL of culture dilution. The suspension was then incubated at 30ºC in an anaerobic jar. Individual colonies that developed were picked and cultured in the corresponding culture medium. The process of isolation was repeated several times until isolates were deemed to be pure. Genomic DNA was extracted according to the protocol described for the Wizard Genomic DNA purification kit (Promega). 16S rRNA genes were amplified by using primers Fd1 (5'-AGAGTTTGATCCTGGCTCAG-3') and Rd1 (5'-AAGGAGGTGATCCAGCC-3') and by using the following reaction conditions: 1 min at 94ºC, 30 cycles of 30 s at 94ºC, 1 min at 50ºC and 2 min at 72ºC, and a final extension step of 10 min at 72ºC.

PCR fragments were then cloned into pGEM-T-easy (Promega). Recombinant clones, with inserts of the correct length, were sequenced by using primers SP6 (5'-ATTTAGGTGACACTATAGAA-3') and T7 (5'-TAATACGACTCACTATAGGG-3') (Genome Express). The nucleotide sequences of the 16S rRNA genes were compared with reference sequences from the GenBank database. The 16S rRNA gene sequences of the strains were aligned with reference sequences of various *Desulfovibrio* species using programs provided by the Ribosomal Database Project II. Sequence alignment was verified manually using the program BIOEDIT. Positions of sequence and alignment uncertainty were omitted from the analysis. Pairwise evolutionary distances based on an unambiguous stretch of 1274 bp were computed by using the Jukes and Cantor (1969) method. The dendrogram was constructed by

using the neighbour-joining method. Confidence in the tree topology was determined by bootstrap analysis based on 100 re-samplings.

Scanning Electron Microscopy

Surface morphology of the present SRB culture was studied by the scanning electron microscope (SEM). SRB culture samples were filtered through a 0.22µm filter to obtain the cells. Filtered SRB cells were first fixed overnight in 2.5 % glutaraldehyde in 0.1M phosphate buffer (pH 7.0) solution. The fixative solution was decanted off and cells were then washed twice in phosphate buffer (0.1M, pH 7.0) for 10 minutes. Thereafter, the cells were dehydrated in a series of ethanol solutions, 30%, 50%, 70%, 80%, 90%, and twice in absolute ethanol, and each step lasted for 15 minutes. The samples were then dried in liquid CO_2 for 2 hours at critical point (31.1° and 73 atmospheres). Pieces of the membranes containing dried cells were cut into small squares and then mounted on stubs with double-sided tape, and then gold-coated for 30 minutes in a Large Desk II Cold Sputter Etch Coater. The prepared samples were then observed under a JEOL-JSM-840 scanning electron microscope.

Potentiometric titrations

Acid/base properties of SRB cells with regard to H^+ and OH^- ions were studied by potentiometric titrations. The titrations were performed using an automated titration system comprising of a burette system, glass electrode and a pH meter (Metrohm 718 STAT-Titrino model) according previously published procedures (Fein et al., 1997; Cox et al., 1999; Martinez et al., 2002; Ngwenya et al., 2003; Borrok and Fein, 2005; Johnson et al., 2007). Prior to titration, 0.3g (wet weight) SRB cells were suspended in 25 mL of the appropriate electrolyte solution which had been purged by N_2 bubbling for 60 minutes to eliminate CO_2. The suspension was immediately placed into a sealed titration vessel with continuous stirring at 140 rpm under N_2. Titrations were carried out by the gradual addition of pre-set small volumes of 0.1M NaOH or 0.1M HCl titrant (standardized against reagent grade $KC_8H_4O_4H$ and Na_2CO_3 respectively). The titrator was set to add successive base or acid after a stability of 0.1Mv/sec was attained. Three sets of duplicate SRB suspensions were first titrated with 0.1M HCl to about pH 4 and then titrated up to about pH 10 with 0.1M NaOH. SRB titration experiments were conducted at different ionic strengths (0.01M, 0.1M and 0.5M $NaNO_3$) and temperatures (5°C, 50°C and 75°C). A total organic carbon

(TOC) analysis was conducted on the bacterial suspensions to confirm the presence or absence of organic exudates, due to cell lysis. Blank titrations devoid of SRB cells were also performed for base and acid titration. Reversibility of the SRB acid/base behaviour was established by performing reverse titrations.

Fourier Transform Infrared Spectroscopy

The acid/base characterization was complemented by Fourier Transform Infra-Red (FTIR) spectroscopy analysis to confirm the presence of different cell wall functional groups. FTIR analysis of SRB cells was conducted according to a method described by Ojeda et al. (2008). The SRB cells equilibrated with a neutral (pH 6.5) electrolyte solution 0.1M $NaNO_3$. Triplicate SRB cell suspensions (in minimal volume of the electrolyte solution) were initially frozen at -20ºC and then freeze-dried. FTIR spectra of the freeze-dried samples of SRB were recorded on KBr pellets at room temperature using a Perkin Elmer FTIR GX spectrum 2000 (PerkinElmer, USA). The sample compartment was flushed with dry air to reduce interference of H_2O and CO_2. Data analysis focused on the 600-4000 cm^{-1} region.

3.8.2 Total Organic Carbon (TOC) Analysis

Total organic carbon analyses of samples were performed in accordance with Standard Methods of Examination of Water and Wastewater (APHA, 1994). Bacterial suspensions (100 mL) at different pH values (2-11), were centrifuged and the supernatant passed through 0.22µm filters to remove the microbial component. To prevent any organic compound losses, the clear extracts were stored in the dark at −20°C for not longer than 7 days until analysis time. The analysis of dissolved organic carbon was performed by means of a Shimadzu TOC-5000/5050 analyzer coupled to an ASI-V autosampler (Shimadzu Scientific Instruments, Inc., Tokyo, Japan). TOC analysis was performed using the 'acidify and sparge' method, otherwise known as Non-Purgeable Organic Carbon (NPOC) method. An overview of the instrument specifications and basic operation conditions used for TOC analysis is shown in Appendix 1. During the NPOC analysis, the sample is automatically injected into the total carbon reactor along with an oxidising agent (1.69 M $Na_2S_2O_8$) and, with 5% H_3PO_4 (v/v) to adjust the sample pH to 2-3. After pH adjustment, sparge gas is bubbled through the samples for 3 minutes to eliminate the inorganic carbon component. The total carbon remaining in the sample after sparging is

measured to determine the total organic carbon. The TOC concentration of the samples was estimated for a calibration curve constructed using potassium hydrogen biphthalate (KHP) working standard solutions with an organic carbon range of 2-12 mg/L. The zero standards (blanks) were prepared using Ultrapure Mill-Q water. All samples were analysed in duplicate.

3.8.3 Solid Phase Sr, Co And Cs Precipitates Analysis

Speciation Analysis

To determine the species distribution of the solid phase metal species, the bound metals were released from the SRB biomass using different desorbing agents of varying strengths according to a method by Tessier et al. (1979). SRB cells in aqueous solution not spiked with a metal served as a control.

Step I: To extract exchangeable species, 8 mL of 1M $MgCl_2$ solution (pH 6) was added to 2 g of the pellet obtained by centrifugation (7000g × 15 minutes). The mixture was stirred at 25ºC for 1 hour. The mixture was then centrifuged and the supernatant was used for metal analysis.

Step II: To extract species bound to carbonates, 10 mL of 0.1M sodium acetate adjusted to pH 5 using acetic acid was added to the residue obtained at step I. The mixture was stirred at 25ºC for 3 hours, and then centrifuged and the supernatant was used for metal analysis.

Step III: To extract species bound to oxides, 10 mL of 0.1M Hydroxyl ammonium chloride (pH 2) was added to the residue obtained from step II. The mixture was also stirred at 96ºC for 3 hours, and then centrifuged and the supernatant was used for metal analysis.

Step IV: To extract species bound to sulphide, 5 mL of 30% hydrogen peroxide adjusted to pH 2 with HNO_3 and 3 mL 0.02M HNO_3 was added to the residue obtained from step III. The mixture was stirred for 2 hours at 85ºC. This was followed by the addition of 5 mL aliquot of 3.2M ammonium acetate (pH 2) in 20% (v/v) HNO_3 to avoid adsorption of the extracted metal into the oxidized fraction. The mixture was stirred for a further 30 minutes at 85ºC and then centrifuged and the supernatant was used for metal analysis.

Step V: To extract residual strontium species, 2 mL each of H_2O_2, HNO_3 and Hydrofluoric acid were added to the residue obtained from step IV. The mixture was stirred at 96ºC for 3 hours, and then centrifuged and the supernatant was used for metal analysis.

3.8.4 Metal Concentration Analysis

Strontium

Total, solid-phase and dissolved Sr^{2+} concentrations were determined separately. Raw samples were centrifuged at 10 000 g for 20 minutes to obtain the dissolved and solid phase fractions. To determine the dissolved Sr^{2+} concentration, 2.5mL of the supernatant was dispensed into 10mL acid washed tubes to which 0.5mL of 30% H_2O_2 and 0.1mL of 70% trace metal grade HNO_3 were added and incubated at 60°C overnight. The resulting pellet was also subjected to the same acid digestion treatment. Following digestion or extraction, the volume of the solution was made up to 10mL, giving a 4× dilution factor. Strontium concentrations were determined at a wavelength of 460.7 nm in a nitrous oxide-acetylene flame using an AAnalyst400 Perkin Elmer AAS (Perkin Elmer, Shelton, USA) equipped with a 10 mA hollow cathode Sr lamp. Prior to sample analysis, the instrument was calibrated against a calibration and reagent blank (5% nitric acid solution in ultrapure water), as well as Sr^{2+} standards containing 0.2, 0.4, 0.6, 0.8, and 1.0 mg Sr/L). Linear calibration graphs were obtained over the concentration ranges 0–1.0 mg/L , with the correlation coefficient set at not less than 0.995 ($R^2 \geq 0.995$). Strontium ionization in this flame was suppressed by the addition of a potassium chloride solution to give a final concentration of 2 mg/L K^+ in all samples including the standards and blank. The lower detection limit for this procedure is estimated to be about 20 µg/L.

Cobalt

Total, solid-phase and dissolved Co^{2+} concentrations were also determined as described previously for Sr^{2+}. Cobalt concentrations were determined at a wavelength of 240.7nm in an air-acetylene flame using an AAnalyst400 Perkin Elmer AAS (Perkin Elmer, Shelton, USA) equipped with a 10mA hollow cathode Co lamp. Prior to sample analysis, the instrument was calibrated against a calibration and reagent blank (5% nitric acid solution in ultrapure water), as well as Co^{2+} standards of known concentrations. Linear calibration graphs were obtained over

the standard concentration ranges, with the correlation coefficient set at not less than 0.995 ($R^2 \geq 0.995$).

Cesium

Total, solid-phase and dissolved Cs^+ concentrations were also determined as previously described for Sr^{2+}. Cesium concentrations were determined at a wavelength of 852.1 nm in an air-acetylene flame using an AAnalyst400 Perkin Elmer AAS (Perkin Elmer, Shelton, USA) equipped with a 10 mA hollow cathode Cs lamp. Prior to sample analysis, the instrument was calibrated against a calibration and reagent blank (5% nitric acid solution in ultrapure water), as well as Cs^+ standards of known concentrations. Cesium ionization was also suppressed by the addition of a potassium chloride solution to give a final concentration of 2 mg/L K^+ in all samples including the standards and blank. Linear calibration graphs were obtained over the standard concentration ranges, with the correlation coefficient set at not less than 0.995 ($R^2 \geq 0.995$). The lower detection limit for this procedure is estimated to be about 0.005µg/mL.

3.8.5 Sulphate Concentration

The concentration of sulphate was determined using the turbidimetric method (APHA, 1994). Prior to analysis, samples were centrifuged (10 000 g for 15 minutes) to remove suspended solids. To a 5mL sample, 0.25mL of conditioning reagent (consisting of 50mL glycerol, 30mL concentrated HCl, 75g NaCl, 100mL ethanol and 300mL deionized water) was added, and mixed thoroughly. After that an excess amount of finely ground $BaCl_2$ was added and mixture was homogenized in a vortex for 1 minute. The absorbance of the mixture was measured at 420 nm. Sulphate concentration was calculated from a calibration curve ($R^2 \geq 0.995$) obtained from measurement of standard sulphate concentration in the range 2-20 mg/L, using a similar procedure for sulphate analysis.

3.8.6 Biomass Concentration

Viable SRB population

The three-tube most probable number (MPN) method was used for estimating the viable SRB population. Samples were first serially diluted by aseptically transferring 1 mL volumes into rubber-sealed culture tubes containing 9mL Postgate medium C. The culture tubes were then

incubated in the dark at 37℃ in a shaker at 200rpm for up to 28 days. Blackening of the medium due to FeS formation was regarded as a positive growth result. After the 28 days of incubation, the pattern of positive and negative tubes per dilution is noted, and then an MPN calculator was used to determine the most probable number of organisms.

Total SRB cell counts

The total bacteria count (TBC) method was used to estimate the total bacterial population. Bacteria were enumerated by direct counting using a Petroff-Hausser Counting Chamber (Labotech, South Africa) on a phase contrast Zeiss Axioskop II microscope (Zeiss, Germany).

Bacterial density (g dry/L)

For dry biomass determination, bacterial suspension aliquots of 30 mL were passed through a pre-weighed 0.22µm milli-pore filter. Prior to use, the filter was rinsed in ultrapure water to remove soluble salts that might be present in the filter. The biomass accumulated on the filter was dried at 80ºC for 48 hours and then weighed.

CHAPTER 4

Sr^{2+}, Co^{2+} and Cs^{+} REMOVAL IN A BATCH SULPHIDOGENIC BIOREACTOR

4.1 PROSPECTS OF RADIONUCLIDE REMEDIATION IN AN SRB BIOREACTOR

The present study evaluates the applicability of an SRB biomass as the reactive component in a metal bioremediation system aimed at controlling radionuclide dispersion in the environment. Due to their metabolic activities (which result in the production of biogenic ligands), reactive surface properties and ubiquitous distribution, SRB are considered to be principal microbial agents for controlling the dispersion of metals and radionuclides in the environment (Lovley and Phillips, 1992; Lloyd et al., 1999; Smith and Gadd, 2000; Ngwenya and Whitely, 2006). While the utilisation of SRB cultures for the bioremediation of water sources contaminated with Sr^{2+}, Co^{2+} and Cs^{+} as the ultimate solution is not completely fulfilling, however, it is the only practical solution worth exploring, considering that these microorgansisms have been found to be capable of surviving in irradiated environments (Bruhn et al., 2009). Engineered bioremediation (through biostimulation and bioaugumentation) has, in some instances been proposed as a potential strategy for the immobilization of various environmental contaminants in groundwater systems (Brown et al., 2006). However, the application of active (or growing) microbial cultures to contaminated sites is often complicated by unpredictable microbial activities due to the toxic effects of the metals and radionuclides. In addition, fluctuations in environmental conditions further present uncertainties in the performance of the culture in the contaminated environment.

Therefore, it is critical that the growth, metabolism and diversity dynamics of prospective metal bioremediation bacteria is thoroughly evaluated under contaminated environmental settings. In such cases, kinetic models for bacterial growth and biological substrate consumption become valuable aids for the design, operation and control of the chosen bioremediation strategies. Furthermore, the models become valuable research tools to improve our understanding of the fundamental microbial processes and interactions during metal bioremediation. According to

Mazidji et al. (1992), the broad non-specific impact of metals on microbial activity is manifested through two distinct modes of action; mortality of less tolerant bacterial species, leading to a decrease in total number of bacterial population and diversity, and the reduction of metabolic activities of the surviving bacterial culture. The former can be defined as the toxic effect of the metal, while the decrease in metabolic rate reflects the inhibitory effect of the metal. The present study presents findings on the toxic and inhibitory effects of Sr^{2+}, Co^{2+} and Cs^{+} on an SRB consortium by monitoring the changes in microbial diversity, biomass population and the sulphate reduction rates.

4.2 SRB CHARACTERIZATION AND SCREENING

4.2.1 Partial Characterization of the Initial SRB Consortium

In this study, a number of approaches were used to characterize the SRB consortium before and after exposure to increasing Sr, Co and Cs concentrations in a sulphidogenic bioreactor. Gram staining results indicated that the consortium was predominantly Gram-negative with a few Gram-positive species (Figure 1, Appendix 2). Surface morphology of SRB cells was studied with the scanning electron microscope (SEM). Under the SEM mainly subspherical and rod-shaped SRB cells occurring singly were observed, which is known for lactate as substrate (Figure 2, Appendix 2). The cells were approximately 0.5-1 µm in diameter and 1.7 – 2.5 µm long, which is in close agreement with literature values for SRB (Postgate, 1984; Motamedi and Pedersen, 1998). Phylogenetic analysis using the 16S rRNA fingerprinting technique of the original SRB consortium (control) indicated a dominance of only two genera, belonging to *Enterococcus* and *Staphylococcus* (Figure 4.1). The genus *Enterococcus* belongs to a group of bacteria that comprise of Gram-positive and produce lactic acid as the major metabolic end-product of carbohydrate fermentation. The ability of *Enterococcus* sp. to reduce sulphate into sulphide has been reported. The only difference between these microorganisms and SRB is that *Enterococcus* sp. reduce sulphate to synthesize sulphur containing organic compounds (cystein and methionin metabolism) and sulphide production is highly regulated due to its toxic effect which may contribute to cell death. On the other hand, SRB use sulphate as an electron acceptor to support growth under anaerobic conditions, a phenomenon known as sulphate respiration (Barton, 1992).

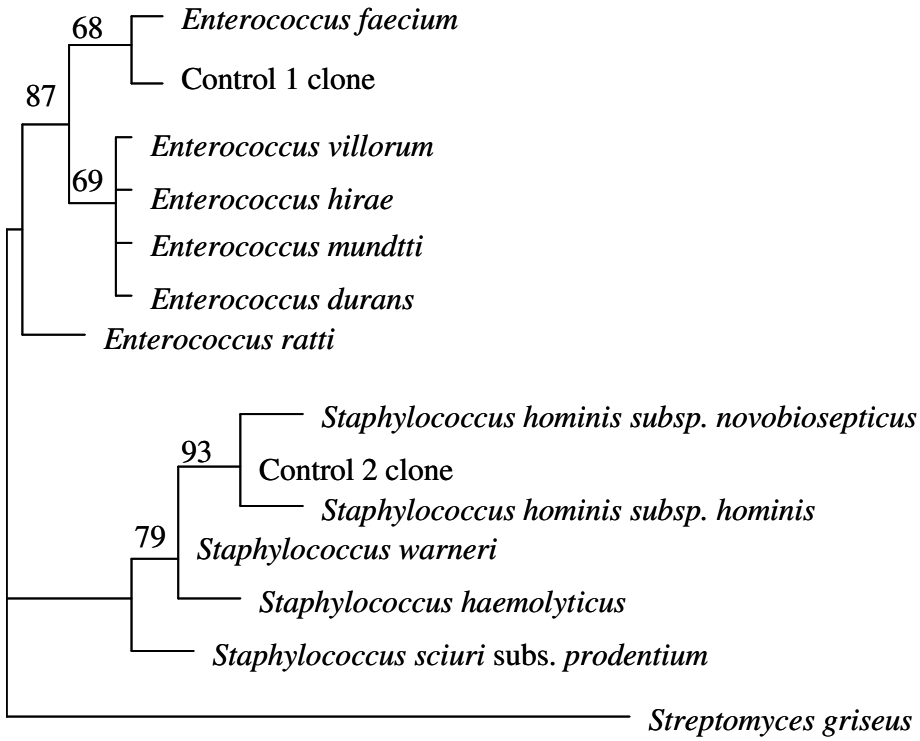

Figure 4.1: Phylogenetic tree of *Enterococcus* and *Staphylococcus* sp. related clones obtained from the original SRB culture (control). The cloned genes are named according to the isolate number.

4.2.2 Microbial Diversity Analysis in the Sr, Co and Cs Bioreactors

A number of researchers have reported the microbial removal of Sr^{2+}, Co^{2+} and Cs^{+} from contaminated aqueous streams (Small et al., 1999; HaiLei et al., 2007; Gao et al., 2010). However, there is lack of knowledge on the probable microbial diversity shifts that occur during Sr^{2+}, Co^{2+} and Cs^{+} bioremediation. Such results can help demonstrate the tolerance as well as applicability of individual microorganisms for selective removal of these metal ions. Previous results obtained from this study indicated that only two genera; *Enterococcus* and *Staphylococcus*, were present in the initial SRB culture, and no significant changes were observed in the SRB culture after a 28 day growth period. However, the presence of Sr^{2+}, Co^{2+} and Cs^{+} in the growth media resulted in the emergence of new bacterial strains representing 3 different genera, belonging to *Citrobacter*, *Paenibacillus* and *Stenotrophomonas* spp.,

respectively. The phylogenetic affiliations and gram-staining results of these isolates obtained from Sr^{2+}, Co^{2+} and Cs^{+} contaminated enrichments with their nearest phylogenetic neighbour in the GeneBank database are shown in Table 4.1. The emergence of these additional bacterial species can be attributed to their tolerance and ability to adapt to conditions of toxic Sr^{2+}, Co^{2+} and Cs^{+} concentrations. A detailed account on the growth and metabolism (sulphate reduction), as well as ability of the bacterial consortia detected in the different bioreactors for Sr^{2+}, Co^{2+} and Cs^{+} removal is presented at a later stage in this chapter.

Table 4.1 Phylogeny of the SRB isolates from Sr^{2+}, Co^{2+} and Cs^{+} contaminated bioreactors.

Clone	*Source*[1]	*Closest Match in GeneBank*[2]	*Similarity (%)*	*Gram staining result*[3]
Control 1	Coal mine wastewater	*Enterococcus faecium*	98	(+)
Control 2	Coal mine wastewater	*Staphylococcus hominis*	100	(-)
Sr1	Sr bioreactor	*Citrobacter* sp.	100	(-)
Sr2	Sr bioreactor	*Citrobacter farmeri*	97	(-)
Sr3	Sr bioreactor	*Citrobacter farmeri*	100	(-)
Sr4	Sr bioreactor	*Citrobacter* sp.	100	(-)
Co1	Co bioreactor	*Enterococcus faecium*	99	(+)
Co2	Co bioreactor	*Paenibacillus motobuensis*	99	(+)
Co3	Co bioreactor	*Paenibacillus motubuensis*	99	(+)
Co4	Co bioreactor	*Paenibacillus motobuensis*	99	(+)
Cs1	Cs bioreactor	*Enterococcus* sp.	99	(+)
Cs2	Cs bioreactor	*Enterococcus faecium*	99	(+)
Cs3	Cs bioreactor	*Stenotrophomonas maltophilia*	99	(-)

[1]Direct from coal mine wastewater or Sr^{2+}, Co^{2+} and Cs^{+} contaminated enrichments.
[2]Based on partial 16S rRNA sequences. Bootstrap = 100.
[3]Based on a method by Shimeld and Rodgers (1999), where (–) = Gram-negative and (+) = Gram-positive .

Microbial Diversity Shifts in the Presence of Strontium

Strontium exists in the environment in a variety of compounds, with the divalent cation, Sr^{2+}, as the most dominant species in contaminated groundwater systems (Brown et al., 2006). The biosorption of Sr^{2+} by bacteria has been reported by Small et al. (1999) and Ngwenya and Chirwa, (2010). However, this is the first study to demonstrate Sr^{2+} tolerance of individual microorganisms in an SRB consortium. Results obtained from this study revealed that cloned 16S rRNA gene sequences of bacterial enrichments obtained from Sr^{2+} contaminated bioreactors were closely affiliated to the marine SRB species belonging to genus *Citrobacter*. Figure 4.2

shows the phylogenetic affiliations of SRB clones isolated from Sr^{2+}contaminated enrichments and some known related bacteria based on partial 16S rDNA sequences. In particular, *Citrobacter farmeri* is a member of family *Enterobacteriaceae*, Gram-negative, obligate facultative and cocci-shaped anaerobe, which grows on lactate, acetate, pyruvate and hydrogen when provided sulphate as an electron acceptor. The ability of the *Citrobacter* sp. for sulphur and sulphate reduction has been reported (Odom and Singleton 1992; Sahrani et al., 2008; Qiu et al., 2010). *Citrobacter* sp. have been isolated from broad range substrate ecologies such as effluents from wastewater treatment plants, soil and aquatic habitats, as well as in microbial communities associated to biofilms that cause corrosion of oil pipelines (Holt et al. 1994; Nada et al. 2004; Neria-Gonzalez et al. 2006). These microorganisms have been used for the removal of a range of metals, including Pb, Cu, Cd, An, Am, U, La, Th (Macaskie and Dean, 1982; Macaskie et al., 1992; Sharma et al., 2009).

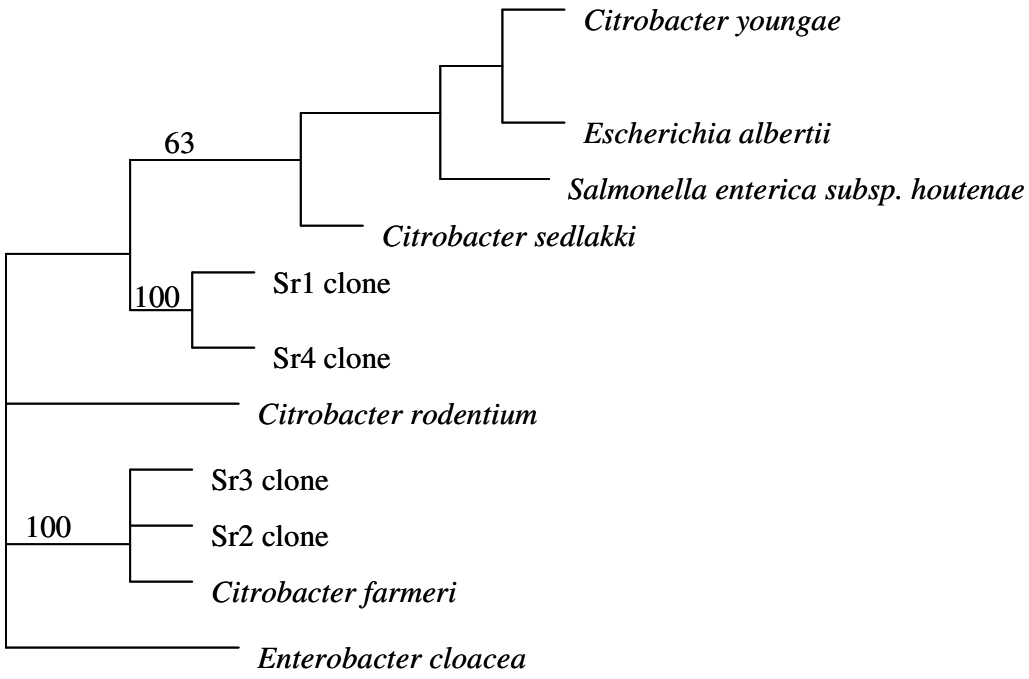

Figure 4.2: Phylogenetic tree of *Citrobacter* sp. related clones obtained from cultures grown in Sr^{2+} contaminated medium. The cloned genes are named according to the source/contaminating metal and isolate number.

Microbial Diversity Shifts in the Presence of Cobalt

The toxic and inhibitory effects of cobalt on the growth sulphate reducers have been studied before, as some SRB require the presence of a cobalt-containing, vitamin B_{12}-methyltransferase for carbon oxidation through the acetyl-CoA pathway (Weijma et al., 2000; Ekstrom and Morel, 2008). Results obtained in the present study indicated that the 16S rRNA gene sequences of SRB clones isolated from Co-contaminated bioreactors were closely related to *Paenibacillus* sp. and *Enterococcus* sp. *Paenibacillus* sp. are Gram-positive, facultative anaerobic bacteria that are related to *Bacilli* but differ in the DNA encoding their 16S rRNA. They have been shown to be capable of utilizing acetate as a carbon source (Nakamura, 1984). The phylogeny of *Paenibacillus* sp. and some known related bacteria based on 16S rDNA sequences are shown in Figure 4.3. The bacterium *Paenibacillus* has also been shown to be able to reduce colourless potassium tellurite to black metallic tellurium (Chien and Han, 2009). Similarly, the Co-reducing capability of these microorganisms has been recently reported by Gao and coworkers (2010).

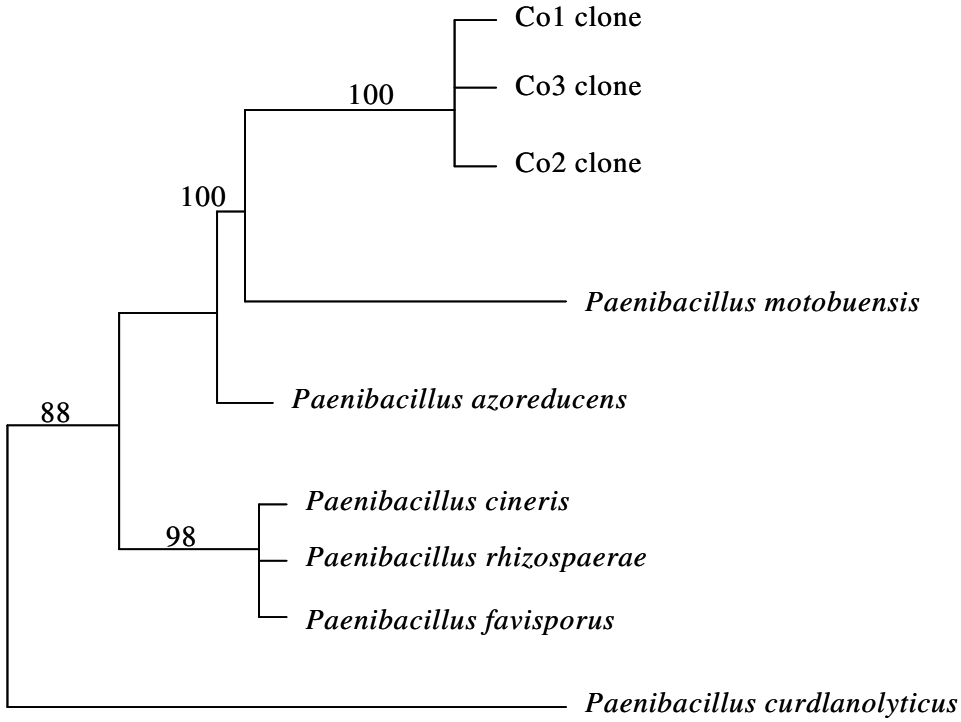

Figure 4.3: Phylogenetic tree of *Paenibacillus* sp. related clones obtained from cultures grown in Co^{2+} contaminated medium. The cloned genes are named according to the source/contaminating metal and isolate number.

Microbial Diversity Shifts in the Presence of Cesium

Phylogenetic analysis of bacterial isolates obtained from sulphidogenic bioreactors contaminated with Cs, indicated that the medium favored the growth of two main strains; *Enterococcus* sp. and *Stenotrophomonas* sp. Figure 4.4 shows the phylogenetic affiliations of the *Enterococcus* sp. isolated from Cs^+ contaminated enrichments and some known related bacteria based on partial 16S rDNA sequences. The biological effects of cesium on different living organisms are well documented (Avery et al., 1993; Lloyd and Macaskie, 2000). However, limited studies have been done on the resilience of individual microorganisms towards cesium. Therefore, results obtained from this study are crucial in establishing the applicability of specific growing bacterial cultures for cesium bioremediation. The observed results demonstrate that *Enterococcus* sp. (original bacterial isolate) is more resilient to Cs^+, compared to *Staphylococcus* sp.

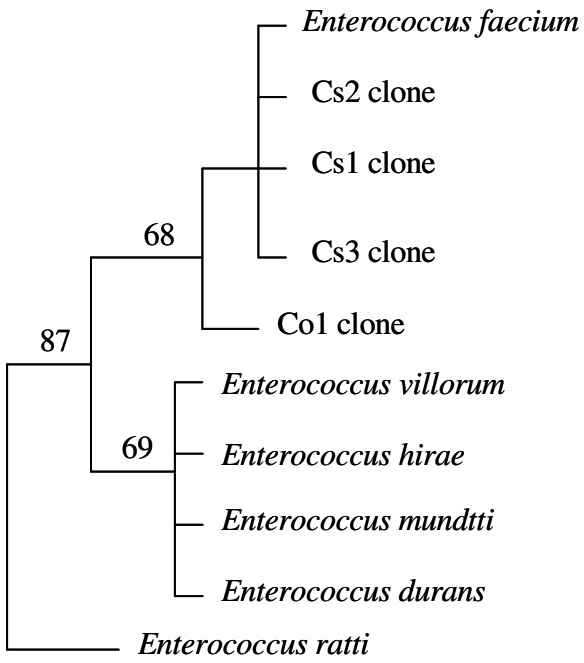

Figure 4.4: Phylogenetic tree of *Enterococcus* sp. related clones obtained from cultures grown in Cs^+ contaminated medium. The cloned genes are named according to the source/contaminating metal and isolate number.

This genus belongs to a group of Gram-positive bacteria, which produce lactic acid as the major metabolic end-product of carbohydrate fermentation. The metal removing capability of the *Enterococcus* sp., particularly, *E. faecium* has been reported recently (Yilmaz et al., 2010). The genus *Stenotrophomonas*, which is phylogenetically placed in the γ-Proteobacteriacea group, was first described with the type species *S. maltophilia*1. The phylogenetic affiliations of the *Stenotrophomonas* sp. isolated from Cs^+ contaminated enrichments and some known related bacteria based on partial 16S rDNA sequences are shown in Figure 4.5. *S. maltofilia* is found in diverse environments, including water, soil debris, raw milk, frozen fish and disinfection solutions used in hospitals (Garcia et al., 2002).

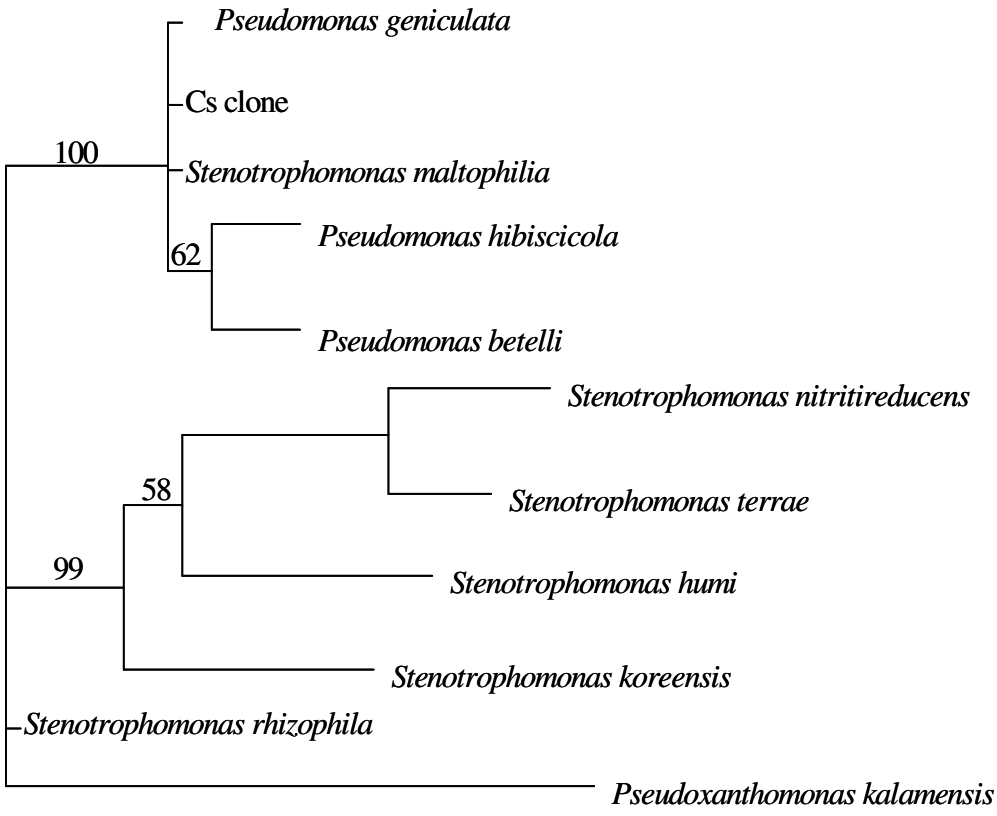

Figure 4.5: Phylogenetic tree of *Stenotrophomonas* sp. related clones obtained from cultures grown in Cs^+ contaminated medium. The cloned genes are named according to the source/contaminating metal and isolate number.

S. maltophilia, has extraordinary range of activities, including the breakdown of natural and man-made pollutants that are central to bioremediation and phytoremediation strategies. Like other Gram-negative bacilli, these microorganisms are tolerant to various toxic metals, such as Ag, As, Cd, Co, Hg, Pb, Zn, U and selenite (Botes et al., 2007; Ryan et al., 2009). Members of the genus *Stenotrophomonas* have also been reported to play an important ecological role in the nitrogen and sulphur cycles (Banerjee and Yesmin, 2002).

4.2.3 Mechanisms of Sr^{2+}, Co^{2+} and Cs^{+} Removal in the Bioreactors

Results obtained from this study showed no metal concentration loss in the absence of bacteria (abiotic control). Experiments were also conducted in a closed bioreactor system, which minimises metal losses/additions to and from the environment. Figure 4.6 shows the distribution of Sr^{2+}, Co^{2+} and Cs^{+} species on bacterial cells after exposure to a medium containing 75 mg/L of each metal. Results obtained suggest that Sr^{2+} removal occurred mainly through biosorption as about 68% of the solid phase Sr^{2+} was found to be occurring in the exchangeable fraction, gives an indication of the amount of Sr^{2+} that is bound to cell surface functional groups by relatively weak electrostatic interaction, and can be released by ion-exchange processes (Dahl et al., 2008). Similarly, high metal concentrations were obtained in the exchangeable fractions of both soil amended with sewage sludge and sulphide-rich tailings of a mine (Nyamagara, 1998; Carlsson et al., 2002). The remainder of the solid-phase Sr^{2+} was a result of a chemical precipitation due to the presence of ligands in the medium, including sulphate (resulting in the formation of insoluble strontium sulphate), as well as products of both sulphate reduction and carbon oxidation. About 22% of the Sr^{2+} was bound to carbonates, 4% bound to oxides and hydroxides, 3% sulphides and the remainder occurring as an immobile fraction. The mechanisms of Sr^{2+} removal by other microorganisms, e.g. *Aspergillus niger* has been studied. The experimental data obtained showed that immobilised *A. niger* was effective in removing Sr^{2+} from aqueous solution. Analysis of the Sr^{2+} precipiates by FTIR analysis showed that Sr^{2+} removal was facilitated by the presence of surface amide groups I and II (Pan et al., 2009). Regardless of the metabolic state of the SRB cells, the results obtained clearly demonstrated that the different bacterial surface chemical functional groups played a significant role in determining the mode and extent of Sr^{2+} removal in the bioreactor. The unique and strong Sr^{2+} complexing ability organic ligands present on the SRB cell surface is detailed in Chapter 5.

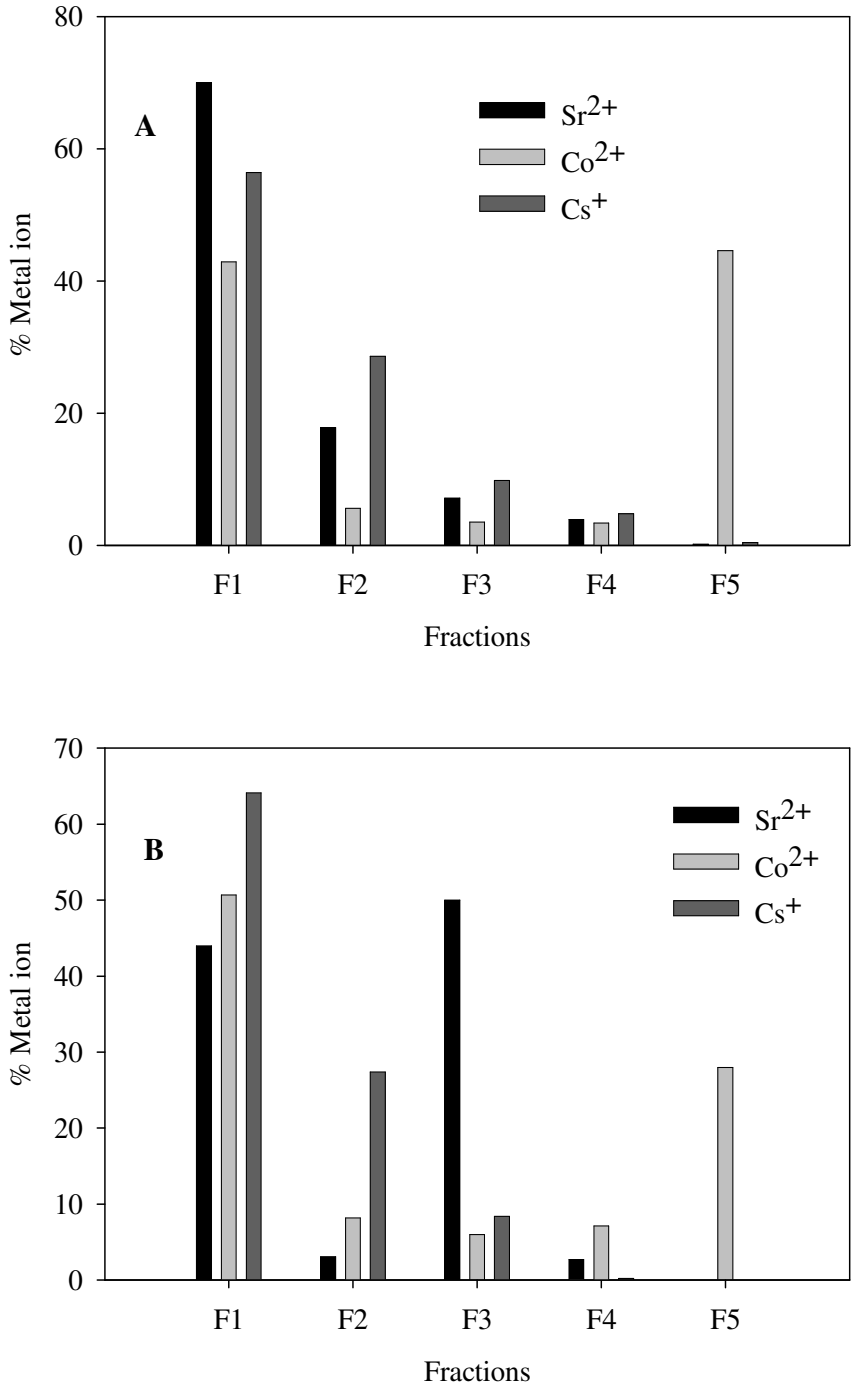

Figure 4.6: Partitioning of Sr^{2+}, Co^{2+} and Cs^{+} species on viable (A) and dead (B) SRB biomass. F1 = exchangeable, F2 = carbonates, F3 = oxides, F4 = sulphide/organics, and F5 = residual fraction.

However, the metabolic state of the bacteria had a significant effect on the mechanism and fate of Co^{2+} in the bioreactor. Under growth conditions, the Co^{2+} in the medium is ultimately accumulated both inside (45%) and outside the cell (43%). The dual mechanism of metal removal from solution by the bacterial cells has been reported before (Ho and McKay, 2000; Aksu, 2001; Goncalves et al., 2007). Initially metal sorption occurs through a rapid sorption phase, where the metal ions bind to the surface through the formation of ionic bonds, which is followed by a slower, metabolism-dependent phase, where the metal is accumulated inside the cell. The extent of Co^{2+} intracellular accumulation and adsorption is represented by the immobile fraction (F5) and the exchangeable fraction (F1), respectively. Cobalt is a metabolically essential metal required by most living organisms, including bacteria. Therefore, most Co-assimilating organisms possess specialized energy-dependent systems, which transport the metal into the cell, resulting in its intracellular accumulation (Ekstrom and Morel, 2008). Similarly, in the present study, bioaccumulation accounted was the main mechanism of Co^{2+} removal by live cultures as compared to the non-viable SRB cultures. The remainder of the Co^{2+} in the medium was removed from solution through the formation of metal-ligand complexes, which was observed, in both live and dead SRB cultures.

The accumulation of cesium by different life forms is well documented (Avery et al., 1993; Lloyd and Macaskie, 2000). Cs^{+} is chemically similar to the biologically essential alkali cation K^{+}, and enters into the cells of biosorbents through K^{+} transporters. Alternatively, in the absence of Cs^{+} transport across membranes, extracellular adsorption of the cation on the cell surface occurs. Similarly, in the present study Cs^{+} uptake from solution by SRB biomass (dead or alive) occurred manly through surface adsorption reactions, as most of the sorbed metal was released by an ionic desorbing agent. The observed extracelluar adsorption of Cs^{+} exhibited by the present culture can be attributed to the ability of the SRB potassium ion transporters to discriminate between the toxic cesium cation and biologically essential potassium cation. The resistance of live SRB cultures for Cs^{+} uptake are also be further demonstrated by the slight differences in the percentage amount of Cs^{+} released by the different desorbing agents, as compared to dead SRB cells. Similar results have been obtained in experiments for the accumulation of cesium by the bacterium *Thermus sp*. TibetanG7 (HaiLei et al., 2007).

4.3 SIMULATION OF SULPHIDOGENIC BIOREACTOR PROCESSES

4.3.1 Modelling Approach

Kinetics of SRB growth and biological sulphate reduction

Batch experiments were conducted to estimate the kinetic parameters associated with SRB growth and metabolism in the presence of increasing Sr^{2+}, Co^{2+} and Cs^{+} concentrations. The approach by Kalyuzhnyi et al. (1998) formed the basis for modeling the kinetics of SRB growth and biological sulphate reduction (BSR) in the bioreactors. The Monod model provides a link between bacterial growth and substrate utilization. According to this model, bacterial growth phenomena can be described satisfactorily with four parameters; two kinetic parameters: the maximum growth rate (μ_{max}) and half velocity concentration (K_s), and two stoichiometric parameters: the yield coefficient ($Y_{x/s}$) and substrate (sulphate) concentration (Kovarova-Kovar and Egli, 1998). Since it is anticipated that the presence of metal ions might have negative effects on SRB cell activities, the Monod was modified by the addition of an inhibition term, I, (Equation 3.3), to incorporate the toxic and inhibitory effects of Sr^{2+}, Co^{2+} and Cs^{+}. The present model neglected cell decay because of the relatively short experimental durations.

Kinetics of Metal Uptake by Microbial Biomass

Results obtained in this study indicated that Sr^{2+}, Co^{2+} and Cs^{+} removal occurred in the presence of both active (alive) and non-active (heat-killed) SRB biomass, and metal ion removal occurred mainly through biosorption processes, with the exception of Co^{2+} where additional metal uptake through bioaccumulation also occurs. During metal uptake, the mobile metal ion (metal ion in solution) concentration is in equilibrium with the immobile metal ion concentration on the bacterial cells. Therefore, a linear relationship is assumed between the two. Thus, the decrease in dissolved metal concentration in the bioreactors was accounted for by a simple pseudo second-order rate law equation (Equation 3.4), incorporating a total biomass term (X) which accounts for both the active (alive) and non-active (heat-killed) SRB biomass in the bioreactors. Since, the sulphate concentration in the bioreactors was typically 2-7 orders of magnitude higher that the initial metal concentration, the formation of insoluble $SrSO_4$ at lower initial Sr^{2+} concentrations was assumed to be minimal.

4.3.2 Model Calibration and Parameter Estimation

Experimental and model data sets (S_0, S, X_0, X, C_{ini}, C and t) were obtained from a study of SRB growth and metabolism in the presence of Sr^{2+}, Co^{2+} and Cs^{+} at various concentrations (25-500 mg/L) in batch experiments, where sulphate, biomass and metal concentrations were measured over time. The model was calibrated using sets of data for each metal at an initial metal concentration of 75 mg/L. Model simulations of bacterial population, biological sulphate reduction and metal removal in the bioreactors were implemented in the computer program for simulation of aquatic systems, AQUASIM 2.0 (Reichert, 1998). The initial conditions and model input values for parameters used for the simulation of SRB bioreactor processes are shown in Appendix 3. Monod kinetic parameters were determined by fitting the experimental data to the equations described in Section 3.5.4 by using a non-linear chi-square method, which minimizes the residual sum of squares between the experimental data and calculated values.

4.3.3 Simulation of SRB Bioreactor Processes in the Presence of Strontium

Kinetics of SRB Growth in the Presence of Sr^{2+}

Table 4.2 shows the optimised Monod kinetic parameters for SRB growth in the presence of increasing initial Sr^{2+} concentrations. Fairly constant kinetic parameters were obtained, indicating that the model was precise in simulating SRB growth in the presence of Sr^{2+} as an inhibitor. Model fits improved with increasing inhibitor (initial Sr^{2+}) concentration, suggesting that the model is more applicable at higher initial Sr^{2+} concentrations where SRB growth inhibition is well defined. Similarly, there a good agreement was observed between the experimental data and model predictions (Figure 4.7). However, the model failed to capture the initial short (24 hours) acclimitisation (lag) phase of the bacterial consortium.

Table 4.2 Optimised Monod parameters for SRB population growth in the presence of Sr^{2+}.

C_{ini} (mg/L)	X_0	μ_{max} (1/h)	K_s (mg/L)	$Y_{x/s}$ (mg/mg)	K_i (mg/L)	χ^2
25	46	0.981	466.9	0.0758	0.616	918.8
75*	48	0.987	466.9	0.0735	0.616	611.5
100	47	0.989	462.4	0.0738	0.616	408.8
300	56	0.986	466.8	0.0749	0.616	298.6
500	48	0.982	466.1	0.0749	0.616	68.8

* = data used for model calibration and parameter estimation

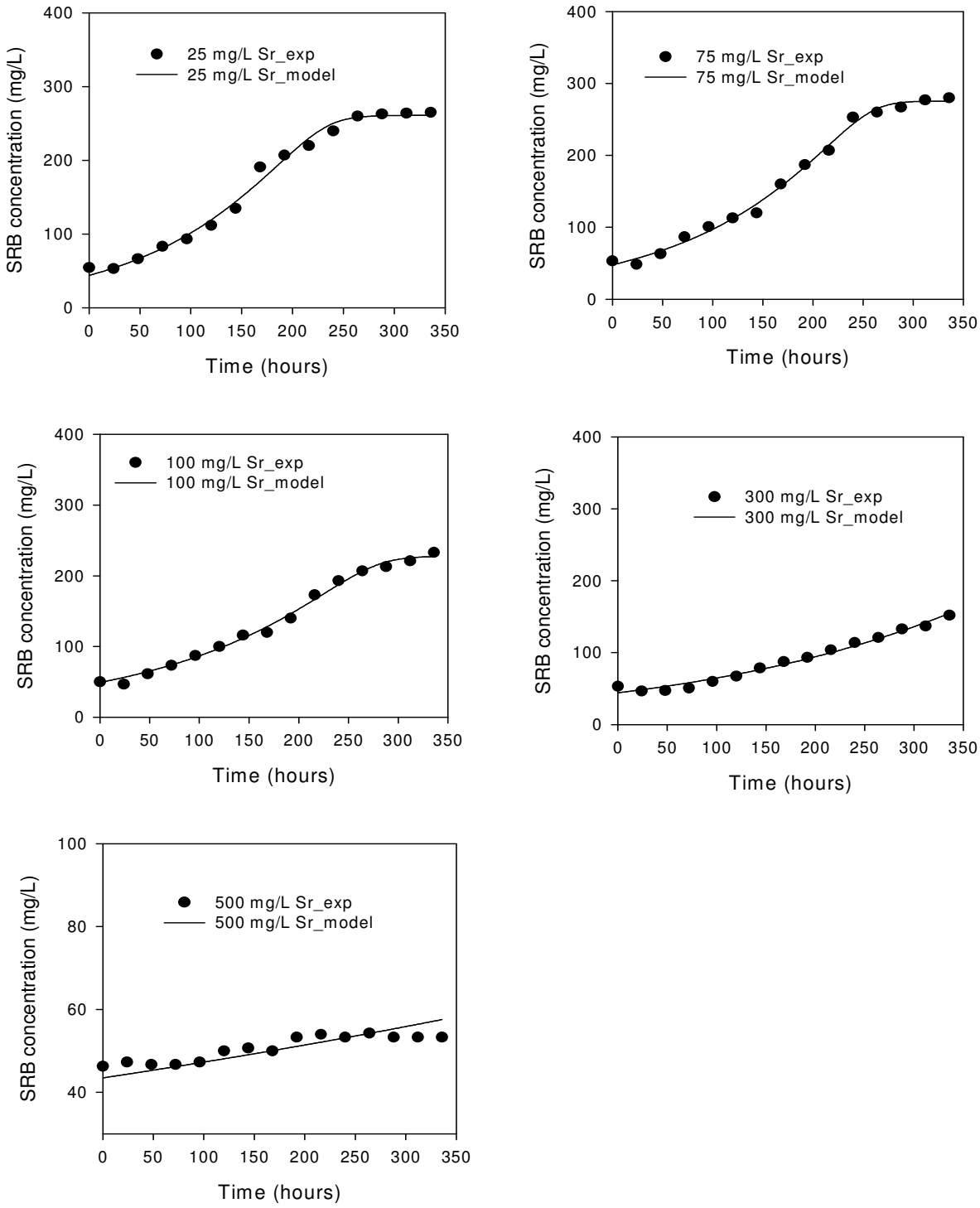

Figure 4.7: Experimental and model predicted growth of an SRB biomass in a batch bioreactor in the presence of different initial Sr^{2+} concentrations.

Both the experimental observations and model simulations indicated that after the short acclimitisation phase, there was a longer exponential phase (up to 250 hours) followed a stationary phase. However, it was evident that increasing the initial Sr^{2+} concentration prolonged the acclimatization phase and delayed the outset of the exponential phase. Generally, the bacterial concentration multiplied remarkably (up to five times) in the presence of Sr concentrations of ≤ 100 mg/L, after which an increase in initial concentration significantly lowered microbial growth. In this case, the toxic and inhibitory effects of the metal were inevitable as neither biosorption nor precipitation lowered the available Sr^{2+} concentration to a level tolerable for SRB growth. Despite the presence of high Sr^{2+} concentrations, it should be noted that despite positive SRB growth was maintained in all bioreactors. However, the SRB biomass growth rate decreased with increasing Sr^{2+} concentrations. These results further demonstrate the resilience of *Citrobacter* spp. towards Sr^{2+}.

Kinetics of Biological Sulphate Reduction in the Presence of Sr^{2+}

Table 4.3 shows the Monod kinetic parameters for biological sulphate reduction in the presence of increasing initial Sr^{2+} concentrations and the corresponding initial SRB concentrations. The obtained goodness of fit (χ^2) values indicate that increasing the initial Sr^{2+}concentration resulted poor model fits. These parameters also suggest that the toxic (growth retardation) effect of Sr^{2+} is well defined compared to its inhibitory effect, as lower inhibition coefficients were obtained for the biological sulphate reduction process. Comparisons between experimental observations and model simulations show marked model misfits (Figure 4.8), which can be attributed to the unpredicted decrease in sulphate concentration due to the chemical precipitation of sulphate (Sr^{2+} reaction with sulphate), which is not accounted for by the present model.

Table 4.3 Optimised Monod parameters for biological sulphate reduction in the presence of Sr^{2+}.

C_{ini} (mg/L)	X_0 (mg/L)	S_0 (mg/L)	μ_{max} (1/h)	K_s (mg/L)	$Y_{x/s}$ (mg/mg)	K_i (mg/L)	χ^2
25	46	3034	0.982	466.9	0.0732	0.354	51864.8
75*	48	3027	0.985	466.6	0.0730	0.356	27400.9
100	47	3013	0.989	466.9	0.0730	0.356	45181.3
300	56	3114	0.988	467.0	0.0735	0.356	99586.5
500	44	2912	0.988	469.0	0.0730	0.357	751165.6

* = data used for model calibration and parameter estimation

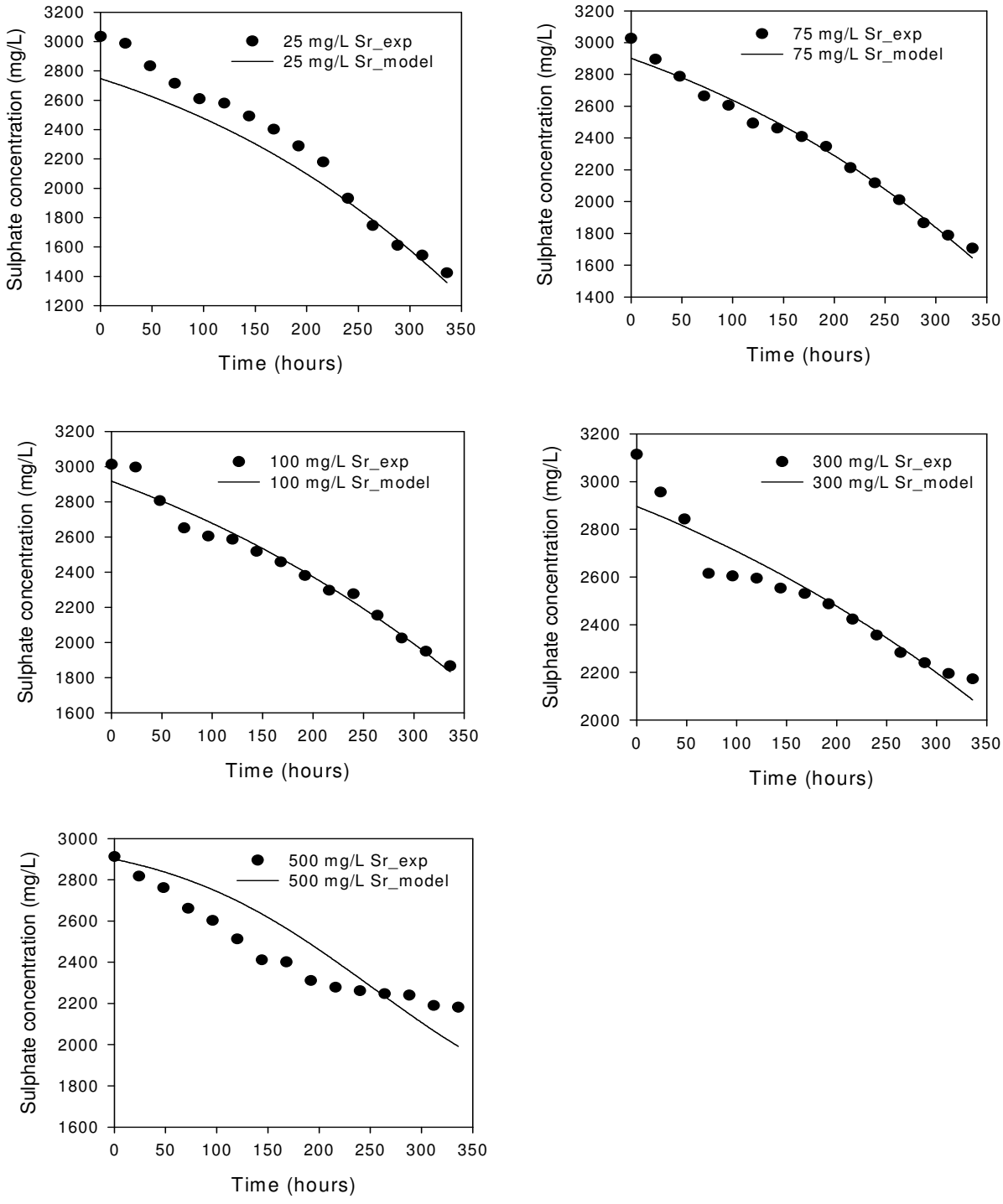

Figure 4.8: Experimental and model simulations of sulphate reduction in a batch SRB bioreactor in the presence of different initial Sr^{2+} concentrations.

The obtained results also reveal that the efficiency of biological sulphate reduction (BSR) was dependent on the initial Sr^{2+} and biomass concentration, where increasing the initial Sr^{2+} concentration resulted in the reduction viable biomass and consequently the metabolic (sulphate reduction) potential of the surviving SRB cultures (previously identified as *Citrobacter* sp.). For example, at an initial Sr^{2+} concentration of 25 mg/L, the sulphate concentration decreased from 3034 to 1501 mg/l, corresponding to a sulphate reduction rate of about 4.56 mg/L/h, compared to a rate of 2.18 mg/L/h observed at an initial Sr^{2+} concentration of 500 mg/L. The sulphate reduction capability of *Citrobacter* sp. is well documented (Odom and Singleton 1992; Barton 1995; Sahrani et al., 2008; Qiu et al., 2010).

Kinetics of Sr Removal in the Bioreactors

The kinetic parameters obtained for the removal of Sr^{2+} (25-500 mg/L) by a growing SRB biomass at biomass initial concentration (X_0) in the range 43.5-56.0 mg/L are shown in Table 4.4. Results obtained indicate that the parameter k_C (rate coefficient) is not a true constant as its value changes with increasing initial concentration. This is not surprising considering that the rate of metal removal from solution is dependent on both the metal and biomass concentration at any given time. High Sr^{2+} concentrations retard SRB growth, consequently limiting Sr^{2+} removal from solution. The model fits improved with decreasing initial metal concentration, implying that the model predictions are more valid for Sr^{2+} uptake at lower initial concentrations. Figure 4.9 shows the uptake kinetics of by the growing SRB biomass, where a comparison is made between the model predictions and experimental observations. The increased difficulties in model fits with increasing initial Sr^{2+} concentrations is a direct result of the premature chemical precipitation of Sr^{2+} due to the formation of $SrSO_4$, as previously reported.

Table 4.4 Optimised kinetic parameters for Sr^{2+} removal by growing SRB cells in a bioreactor.

C_{ini} *(mg/L)*	X_0 *(mg/L)*	k_C *(×10^{-3})*	*Metal removal capacity (%)*	χ^2
25	46	9.73	100	4.73
*75	48	9.88	100	122.4
100	47	2.44	100	1612.1
300	56	0.104	64	73940.1
500	44	0.0111	40	95029.0

* = data used for model calibration and parameter estimation

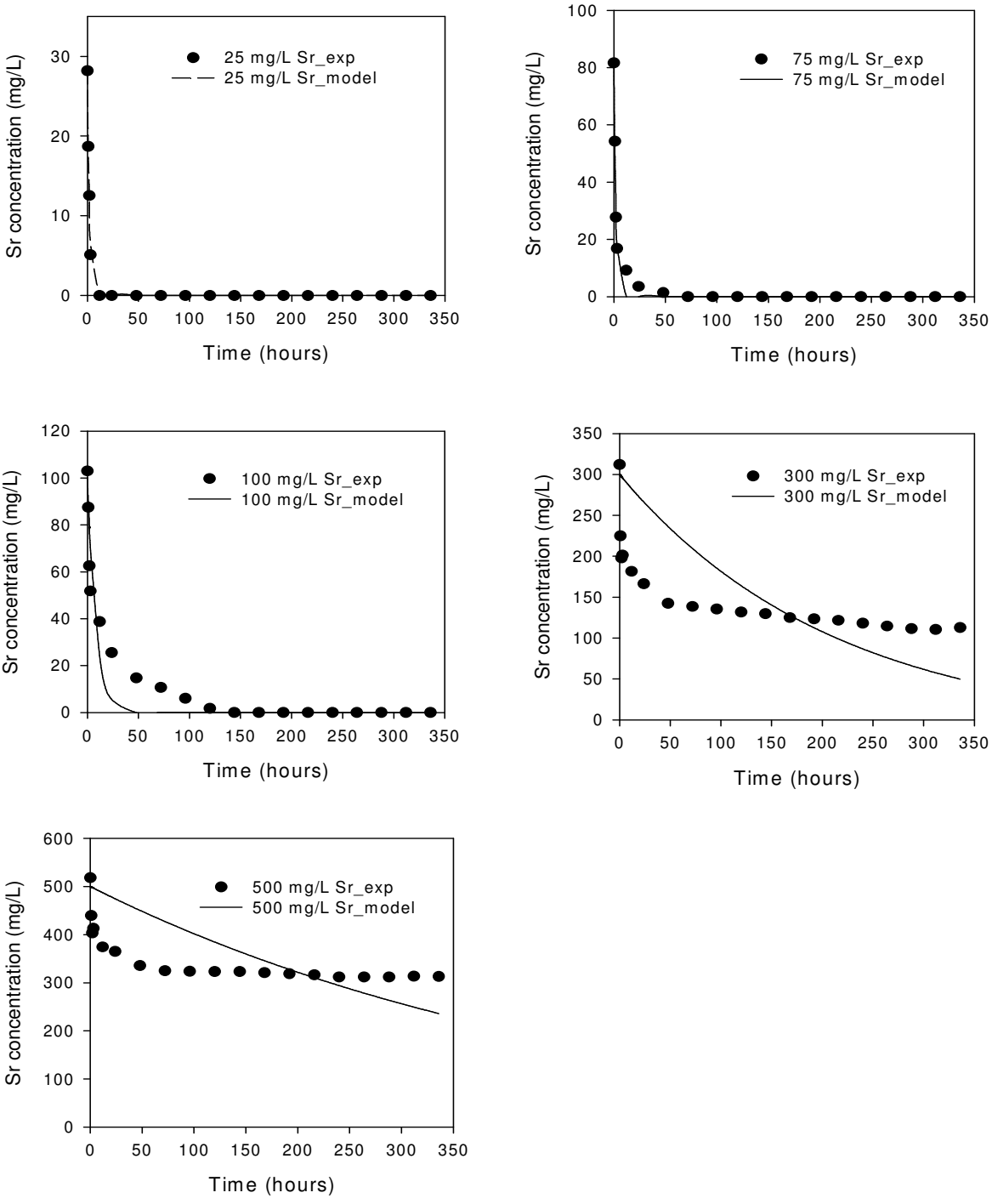

Figure 4.9: Experimental and second-order model plot showing the removal of different Sr^{2+} initial concentrations by a growing SRB consortium in a batch bioreactor.

Generally, in all bioreactors experimental and model simulations an initial fast Sr^{2+} removal rate, which then slows down with time in accordance with the outset of the stationary bacterial growth phase, after which no additional metal removal occurs was observed. This is a common phenomenon for most metal biosorption processes reported in literature (Ho and McKay, 1998; Ho and McKay, 2000; Aksu, 2001). Results obtained also indicated that the overall Sr^{2+} uptake (%) decreased with increasing initial concentration due to increased metal toxicity effects. Complete Sr^{2+} uptake was attained in the first 12, 72 and 144 hours at initial concentrations of 25, 75 and 100 mg/L, respectively. This study is among the first to report on the removal of Sr^{2+} by growing bacterial cultures. Results obtained demonstrate that SRB bioreactors inoculated with active bacterial species belonging to the genus *Citrobacter* hold a promise towards development of *in situ* Sr^{2+} bioremediation technologies.

4.3.4 Simulation of SRB Bioreactor Processes in the Presence of Cobalt

Kinetics of SRB Growth in the Presence of Co^{2+}

Results obtained show that Co^{2+} was less toxic to the present SRB culture compared to Sr^{2+}, as higher maximum growth rates (μ_{max}) and lower growth inhibition coefficient (Ki) was observed (Table 4.5). A good correlation between the experimental data and model simulations was observed, and model fits slightly improved with increasing initial concentration. The effect of cobalt on the growth and metabolism (sulphate reduction) of pure SRB cultures has been studied, where decreased growth rates and metabolic activities were observed in the presence of high Co^{2+} concentrations (Weijma et al., 2000; Ekstrom and Morel, 2008). Similarly, results obtained from this study also show that initial Co^{2+} concentration ≥300 mg/L retarded the growth of the SRB consortium (Figure 4.10).

Table 4.5 Optimised Monod parameters for SRB population growth in the presence of Co^{2+}.

C_{ini} (mg/L)	X_0	μ_{max} (1/h)	K_s (mg/L)	$Y_{x/s}$ (mg/mg)	K_i (mg/L)	χ^2
25	50	1.50	455.0	0.0772	0.352	1810.6
75*	50	1.50	456.2	0.0779	0.358	2182.3
100	50	1.53	456.9	0.0780	0.358	2745.3
300	50	1.51	455.1	0.0780	0.356	2955.5
500	50	1.51	455.1	0.0778	0.358	5534.5

* = data used for model calibration and parameter estimation

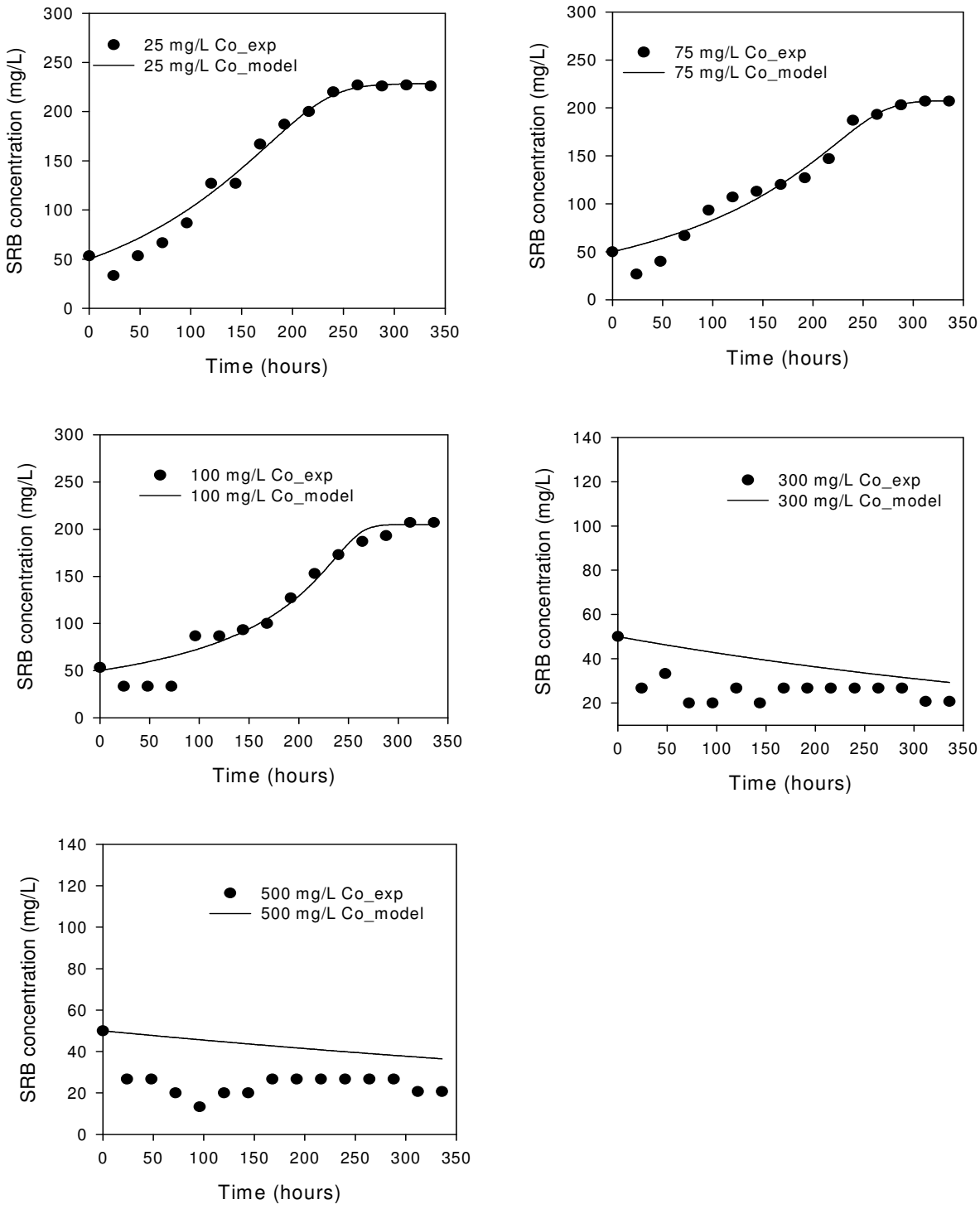

Figure 4.10: Experimental and model predicted growth of an SRB biomass in a batch bioreactor in the presence of different initial Co^{2+} concentrations.

Experimental observations for SRB growth showed that the presence of Co^{2+} in the growth media resulted in a brief initial decline in SRB concentration, which the present model failed to simulate. This phase was followed by a longer exponential phase which lasted up to 250 hours, and lastly a stationary phase, which the were both simulated well by the mode. Generally, positive SRB growth was only recorded at initial Co^{2+} concentrations ≤100 mg/L, after which increasing the initial concentration resulted in growth retardation. Therefore, the poor model simulations observed at higher concentrations (≥300 mg/L) can be attributed to the inadequacy of the model to simulate negative bacterial growth. These results demonstrate the sensitivity of *Paenibacillus* sp. towards high initial Co^{2+} concentrations.

Kinetics of Biological Sulphate Reduction in the Presence of Co^{2+}

Table 4.6 shows the optimised Monod kinetic parameters for biological sulphate reduction by SRB cultures in the presence of increasing initial Co^{2+} concentrations. When the experimental data was fit into the sulphate reduction equation, an improvement in model fit was observed with increasing initial Co^{2+} concentration. The parameters obtained reflect that the inhibitory effect of Co^{2+} on sulphate reduction was less compared to Sr^{2+}, as indicated by the lower sulphate reduction inhibition coefficients. Lower inhibition coefficients (K_i values) were obtained for sulphate reduction, compared to those obtained for SRB growth, suggesting that the toxic (growth retardation) effect of Co^{2+} is superior to its inhibitory effect. This remark is substantiated by experimental sulphate reduction studies at higher initial Co^{2+} concentrations (≥300 mg/L), where positive metabolic activity (sulphate reduction) was observed (Figure 4.11).

Table 4.6 Optimised Monod parameters for biological sulphate reduction in the presence of Co^{2+}.

C_{ini} (mg/L)	X_0 (mg/L)	S_0 (mg/L)	μ_{max} (1/h)	K_s (mg/L)	$Y_{x/s}$ (mg/mg)	K_i (mg/L)	χ^2
25	50	3030	1.50	457.0	0.0779	0.172	44118.3
75*	50	3045	1.50	456.8	0.0778	0.173	14408.7
100	50	3000	1.50	456.1	0.0777	0.172	10297.0
300	50	3030	1.53	455.0	0.0776	0.172	18262.5
500	50	3060	1.50	456.0	0.0776	0.172	16575.6

* = data used for model calibration and parameter estimation

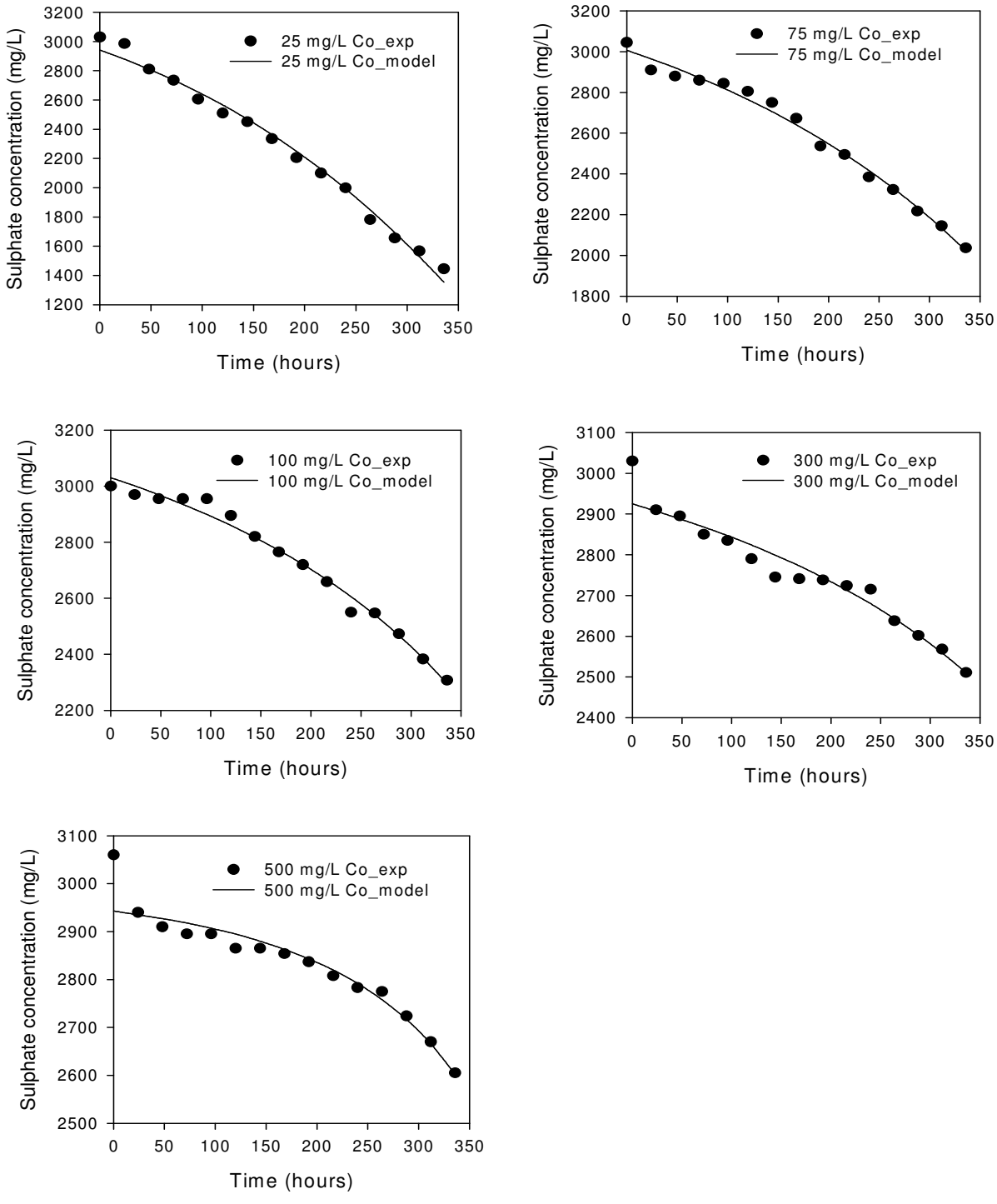

Figure 4.11: Experimental and model simulations of sulphate reduction in a batch SRB bioreactor in the presence of different initial Co^{2+} concentrations.

With regards to metabolic rate efficiency of the consortium, sulphate reduction rates (mg/L/h) of 4.79, 3.93, 3.41, 2.80 and 1.34 were obtained in the presence of 25, 75, 100, 300 and 500 mg/L Co^{2+}, respectively. In view of these findings, it is not clear whether both Co-tolerant bacterial species (*Paenibacillus* sp. and *Enterococcus* sp.) were involved in the observed gradual decrease of sulphate in the bioreactors. While *Paenibacillus* sp. are known to be capable of utilizing acetate as a carbon source (Nakamura, 1984), further studies are necessary to validate their ability or inability to reduce sulphate into sulphide. On the other hand, *Enterococcus* sp., have been shown to be capable of reducing sulphate into sulphide (Barton, 1992). In summary, the underlying prerequisite for successful utilization of active microorganisms for effective Co^{2+} bioremediation is that the initial Co^{2+} should be kept at a minimum.

Kinetics of Co^{2+} Removal in the Bioreactors

Table 4.7 shows the optimised kinetic parameters for Co^{2+} removal by a growing mixed SRB consortium. The goodness of fit (χ^2 values) of the model gradually improved with decreasing initial Co^{2+} concentration. The second-order rate coefficient (k_C) in the range 1-9 was obtained at initial Co^{2+} concentration ≤300 mg/L. However, increasing the initial Co^{2+} concentration to 500 mg/L decreased the rate coefficient, and poor model fit. Accordingly, a lower removal rate was observed at an initial Co^{2+} concentration of 500 mg/L. Generally, the batch experiments showed a 100%, 74%, 69%, 13% and 6% removal of the total Co^{2+} concentration at initial concentrations of 25, 75, 100, 300 and 500 mgL^{-1}, respectively. These results further emphasise that low initial Co^{2+} concentrations have less negative effects on SRB growth and metabolism. Similarly, the experimental data and model simulations also showed that the removal of Co^{2+} by the cultures was dependant on the initial concentration (Figure 4.12).

Table 4.7 Optimised kinetic parameters for Co^{2+} removal by growing SRB cells in a bioreactor.

C_{ini} *(mg/L)*	X_0*(mg/L)*	k_C *(×10^{-5})*	*Metal removal capacity (%)*	χ^2
25	50	8.85	100	135.7
*75	50	4.98	74	212.6
100	50	7.11	69	354.5
300	50	1.44	13	303.0
500	50	0.578	6	494.7

* = data used for model calibration and parameter estimation

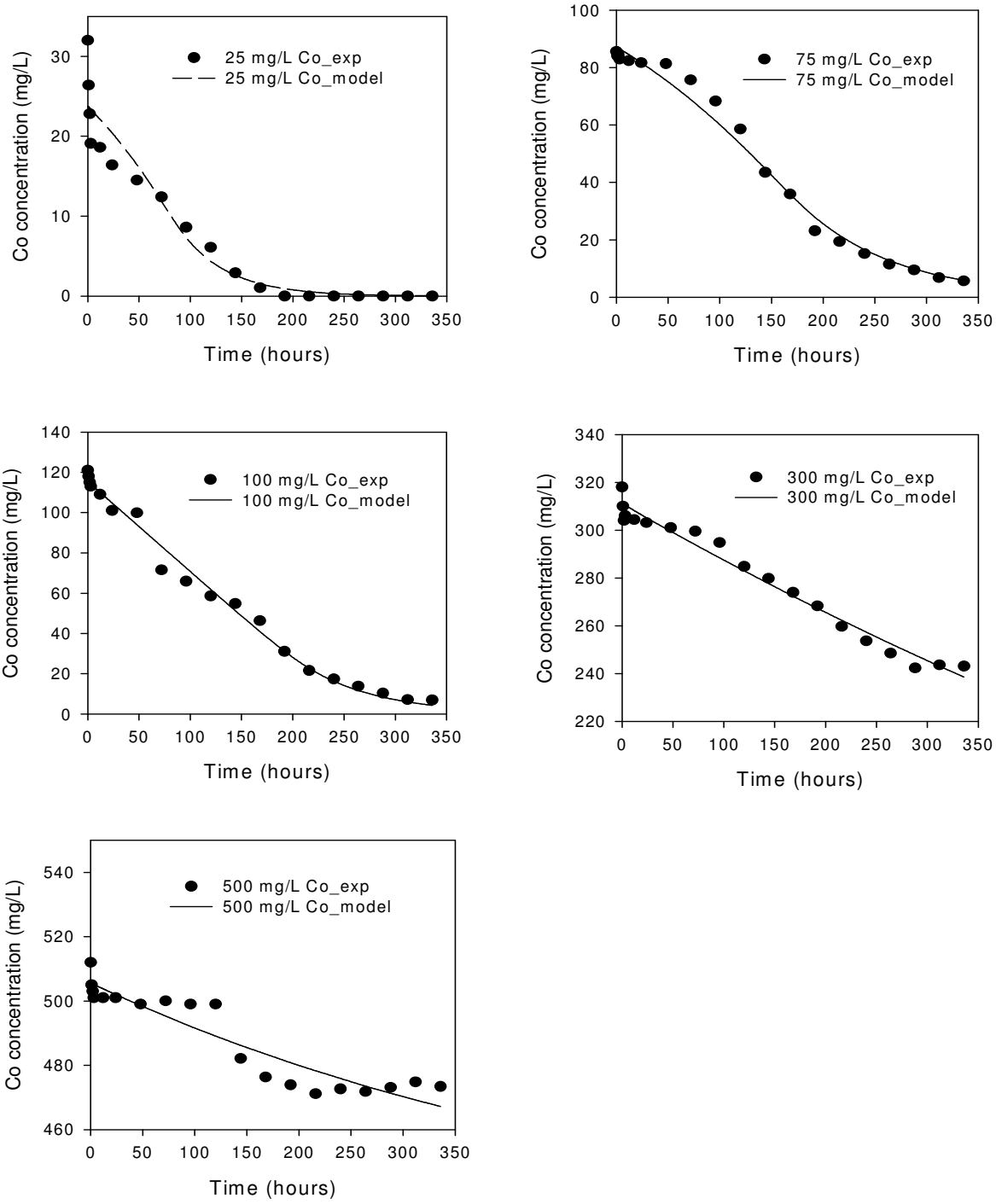

Figure 4.12: Experimental and second-order model plot showing the removal of different Co^{2+} initial concentrations by a growing SRB consortium in a batch bioreactor.

It is evident that increasing the initial Co^{2+} concentration, the Co^{2+} removal capacity of the SRB consortium was lowered to a level corresponding to the observed growth and metabolic activity of the surviving cultures. The removal of Co^{2+} through enzymatic reduction and bioprecipitation (as CoS and $CoCO_3$) in the presence of SRB cultures has been reported (Krumholz et al., 2003). Since SRB possess specialized Co^{2+} assimilation mechanisms, the metal is then ultimately accumulated inside the cell (Weijma et al., 2000; Ekstrom and Morel, 2008; Gao et al., 2010). In accordance with these observations, results obtained in this study indicated that a portion of the Co^{2+} in solution was removed through bioaccumulation. However, in addition to bioaccumulation and biopreciptation, results obtained in this study indicated that a significant portion of the Co^{2+} in solution was removed by biosorption.

4.3.5 Simulation of SRB Bioreactor Processes in the Presence of Cesium

Kinetics of SRB Growth in the Presence of Cs^+

Table 4.8 shows the optimized Monod parameters for SRB growth in the presence of increasing initial Cs^+ concentrations. While parameter optimization was successful, there was no clear trend in the model fits with an increase/decrease in initial Cs^+ concentration. However, the best model fit was obtained at higher initial Cs^+ concentration, suggesting that the present Monod inhibition model is more valid at higher initial Cs^+ concentration (≥100 mg/L) where the toxic effects can be successfully simulated. Lower inhibition (K_i) coefficients were obtained in the presence of Cs^+ in the bioreactors, compared to Sr^{2+} and Co^{2+} suggesting that Cs^+ is less toxic to the SRB consortium. Accordingly, a high maximum specific growth rate (μ_{max}) was observed. At lower initial Cs^+ concentrations (≤100 mg/L), the experimental data obtained suggested that the SRB consortium did not reach stationary phase for the duration of the experiments, while the model predicted that stationary phase was reached after 264 hours of exposure (Figure 4.13).

Table 4.8 Optimised Monod parameters for SRB population growth in the presence of Cs^+.

C_{ini} (mg/L)	X_0 (mg/L)	μ_{max} (1/h)	K_s (mg/L)	$Y_{x/s}$ (mg/mg)	K_i (mg/L)	χ^2
25	47	9.281	492.7	0.0626	0.0571	3008.9
75*	49	9.287	492.8	0.0626	0.0571	720.5
100	47	9.281	492.9	0.0627	0.0571	5518.1
300	49	9.289	492.9	0.0627	0.0571	1254.0
500	55	9.298	492.1	0.0627	0.0572	250.1

* = data used for model calibration and parameter estimation

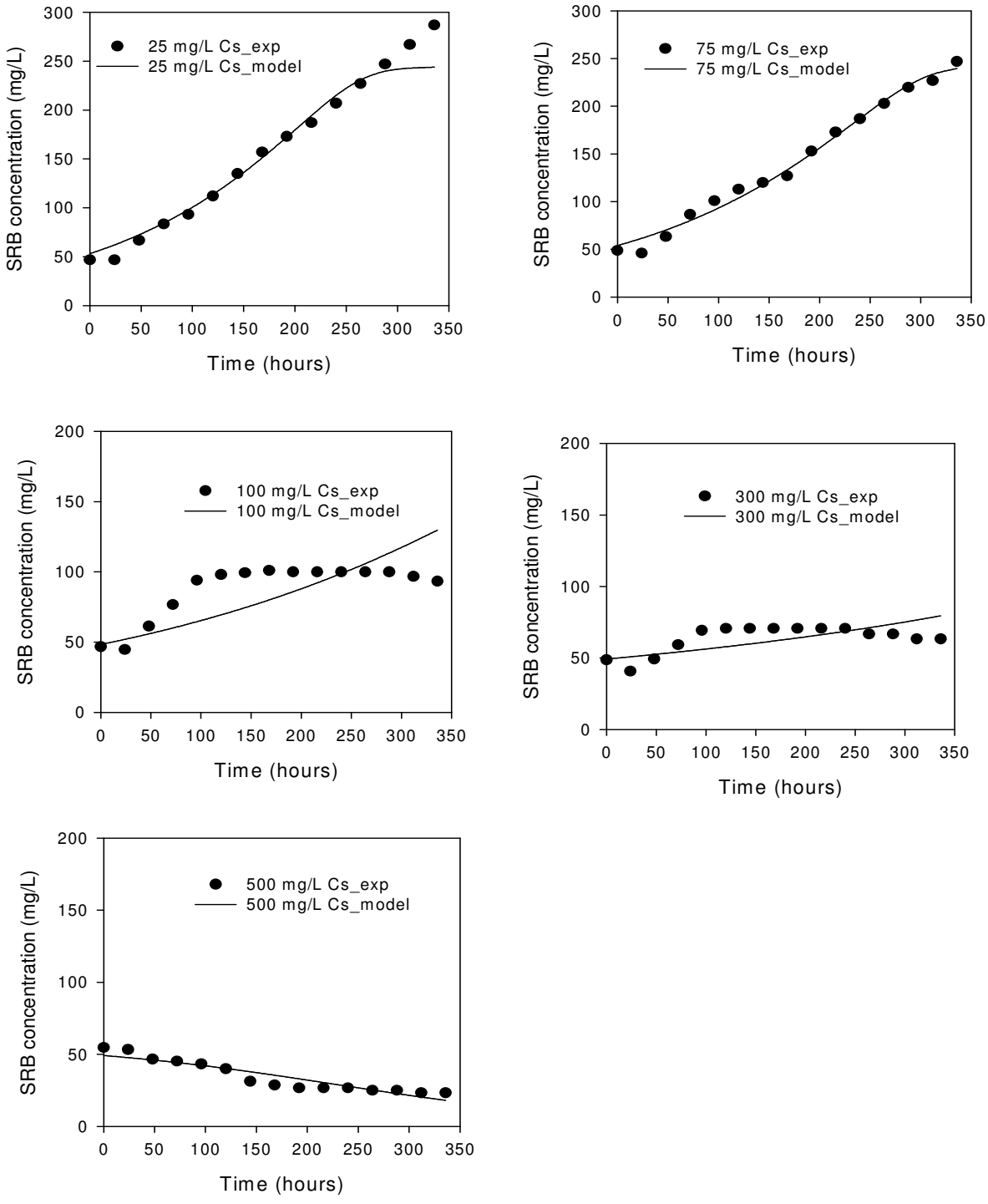

Figure 4.13: Experimental and model predicted growth of an SRB biomass in a batch bioreactor in the presence of different initial Cs^{+} concentrations.

This discrepancy can be attributed to the low toxicity of Cs^+, suggesting that it was not necessary to modify the Monod model with an inhibition term. The low toxicity of Cs^+ towards live microbial cells has been reported. However, its presence in high concentrations can dramatically decrease the uptake of essential growth micronutrients K^+ and Na^+, and these elements, thereby retarding vital microbial processes and growth (Avery, 1995). Therefore, the increased Cs^+ tolerance displayed by the present SRB consortium may result from sequestration of Cs^+ in vacuoles or changes in the activity and/or specificity of transport systems mediating Cs^+ efflux, rendering it less toxic to the microorganisms identified as belonging to *Enterococcus* sp. and *Stenotrophomonas* sp.

Kinetics of Biological Sulphate Reduction in the Presence of Cs^+

Table 4.9 shows optimised Monod parameters for sulphate reduction in the presence of increasing initial Cs^+ concentrations. The obtained results indicate that Cs^+ had a lesser effect on the metabolic activities (sulphate reduction) of the SRB consortium, compared to Sr^{2+} and Co^{2+}, as lower inhibition coefficient (K_i) values were obtained. Model fits improved with increasing initial concentration. However, visual comparisons between the experimental data and model simulations showed a poor correlation, particularly at an initial concentration of 500 mg/L (Figure 4.14). While the experimental data evidently displayed the inhibitory effect of Cs^+ at this concentration, the model predicted a less inhibitory effect. Since Cs^+ is chemically similar to the biologically essential alkali cation, K^+, it enters into the cells of living organisms through the K^+ transporter system. If present in high concentrations, the sequestered Cs^+ can act as a replacement for the essential alkali cation, K^+, thus causing undesirable biological effects on the bacterial cell (Avery, 1995).

Table 4.9 Optimised Monod parameters for biological sulphate reduction in the presence of Cs^+.

C_{ini} (mg/L)	X_0 (mg/L)	S_0 (mg/L)	μ_{max} (1/h)	K_s (mg/L)	$Y_{x/s}$ (mg/mg)	K_i (mg/L)	χ^2
25	47	3034	6.35	499.3	0.0628	0.0283	40115.4
75*	49	3027	9.30	495.0	0.0647	0.0282	17106.0
100	47	3054	9.97	492.7	0.0618	0.0283	10909.7
300	49	3041	9.98	492.4	0.0620	0.0283	9228.5
500	55	3120	9.96	495.7	0.0622	0.0283	8815.4

* = data used for model calibration and parameter estimation

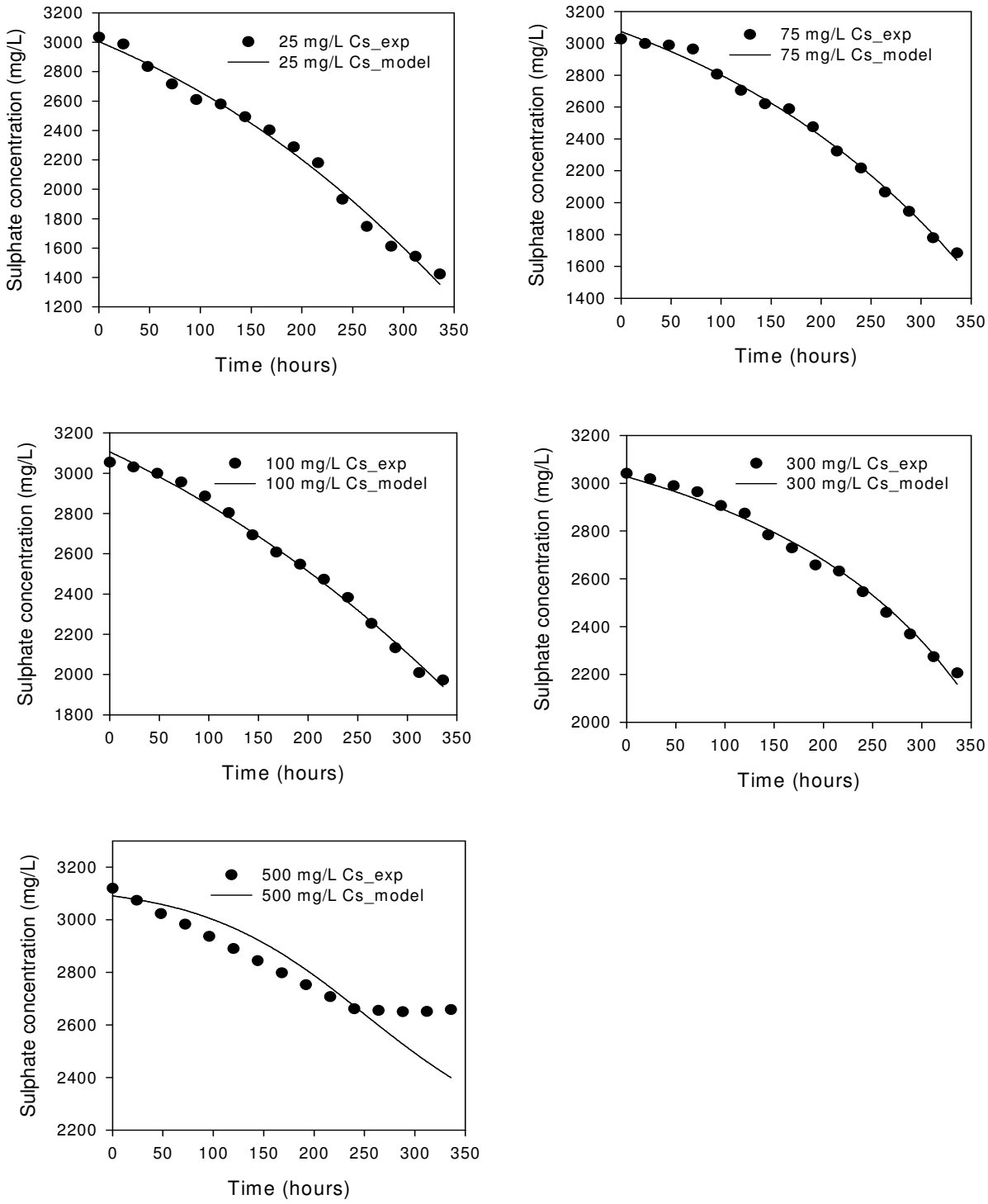

Figure 4.14: Experimental and model simulations of sulphate reduction in a batch SRB bioreactor in the presence of different initial Cs^+ concentrations.

The precise intracellular target(s) for Cs^+-induced toxicity and inhibitory effects have yet to be clearly defined, although certain internal structures, e.g. ribosomes, become unstable in the presence of Cs^+ and Cs^+ is known to substitute poorly for K^+ in the activation of many K^+-requiring enzymes (Avery, 1995). In summary, it can be assumed that the observed reduction of sulphate in the bioreactors was a direct result of the metabolic activities of the two Cs-tolerant isolates, *Enterococcus* sp. and *Stenotrophomonas* sp., due to low toxicity of Cs toxicity. However, the sulphate reduction efficiency of the SRB consortium decreased with increasing initial Cs^+ concentration.

Kinetics of Cs^+ Removal in the Bioreactors

Table 4.10 shows the optimized parameters for Cs^+ uptake by a growing SRB consortium. From this table it is clear that an increase in initial Cs^+ concentration resulted in poor model fits. The parameter, k_C (second-order rate coefficient) and the corresponding Cs^+ removal capacity of the SRB biomass decreased with increasing initial Cs^+ concentration. The low Cs^+ removal capacities at higher (≥300 mg/L) can both be attributed to both the toxic and inhibitory effects of Cs^+, which retard SRB growth and metabolism. Comparisons between the experimental data and model plots indicate that the model satisfactorily simulated removal at initial Cs^+ concentrations ≤75 mg/L (Figure 4.15). At initial concentration ≥300 mg/L, the model predicted a faster rate than was observed in Cs^+ removal experiments. Similarly, there was an evident dependence of Cs^+ removal on SRB concentration. At low initial Cs^+ concentrations of 25 and 75 mg/L, complete removal was observed within the first 24 hours and after 240 hours, respectively.

Table 4.10: Optimised kinetic parameters for Cs^+ removal by growing SRB cells in a bioreactor.

C_{ini} *(mg/L)*	X_0 *(mg/L)*	k_C *($\times 10^{-4}$)*	*Metal removal capacity (%)*	χ^2
25	47	8.00	100	105.7
*75	49	1.33	100	162.1
100	47	0.783	68	1003.4
300	49	0.304	38	3404.9
500	55	0.117	18	6447.5

* = data used for model calibration and parameter estimation

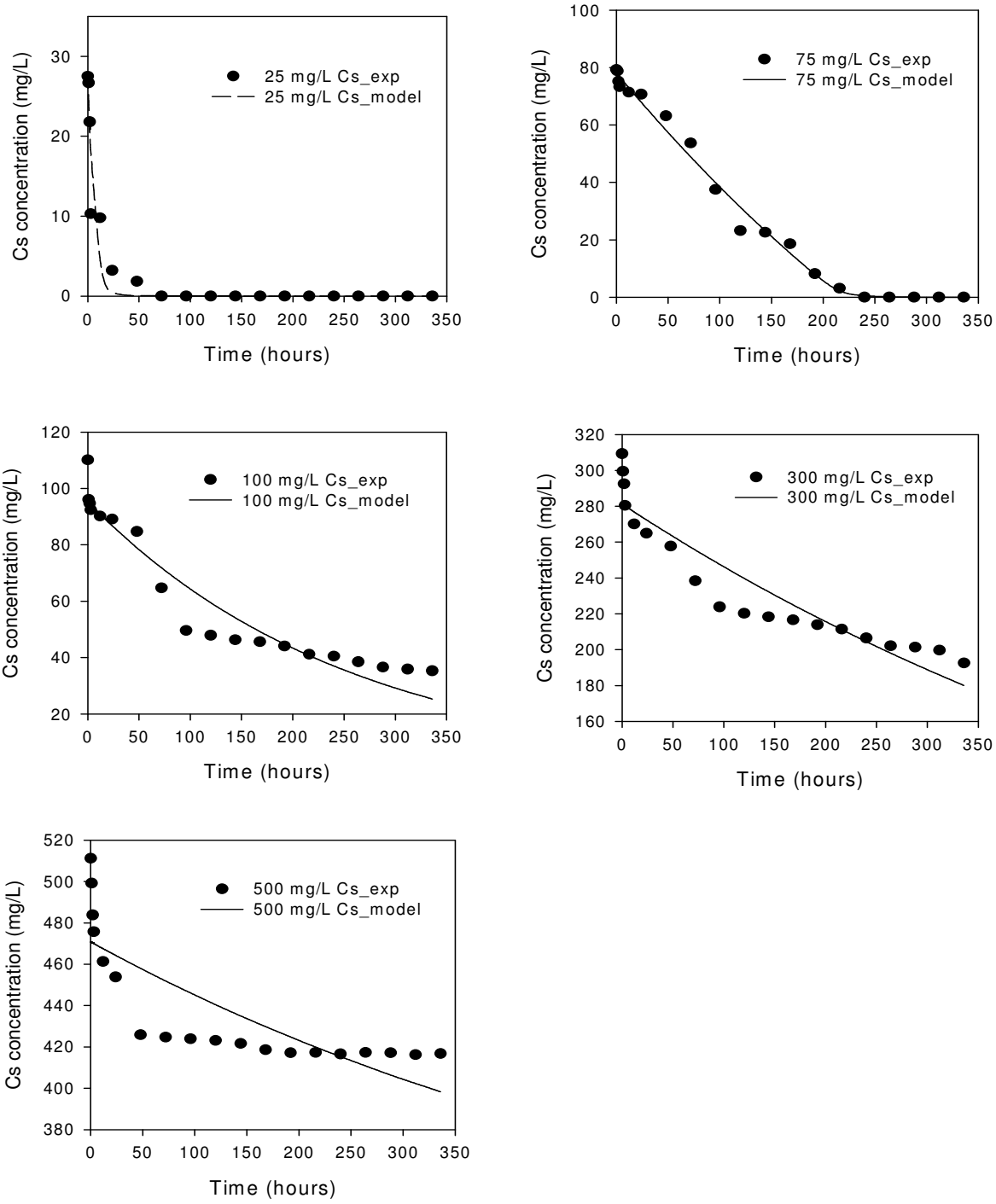

Figure 4.15: Experimental and second-order model plot showing the removal of different Cs^{+} initial concentrations by a growing SRB consortium in a batch bioreactor.

Cs^+ exists almost exclusively as the monovalent cation Cs^+ in the natural environment. Although Cs^+ is a weak Lewis acid that exhibits a low tendency to form complexes with ligands, its chemical similarity to the biologically essential alkali cation K^+ facilitates high levels of metabolism-dependent intracellular accumulation (Lloyd and Macaskie, 2000). However, previous results obtained in this study showed that limited Cs^+ removal bioreactors occurred through bioaccumulation. The low microbial Cs^+ bioaccumulation observed in this study can be attributed to presence of competitive cations, e.g. K^+, Na^+, NH_4^+ and H^+, in the medium, whose presence have been reported to decrease its significantly (Avery, 2004). The distinct chemical properties of Cs^+, indicate that different approaches are required for biological Cs^+ removal to those which are generally adopted for other metals/radionuclides. However, its low toxicity eliminates one potential problem in the use of live/growing cells for its removal. The inherent differences in Cs^+ uptake capacities of different microorganisms appear to be largely attributable to differences in the affinity of monovalent cation transport systems for Cs^+. The application of rigorous screening procedures involving the use of autoradiography has great potential for isolation of microorganisms with particularly high affinities for Cs^+ (Avery, 1995).

4.3.6 Sensitivity Analysis

The sensitivity test, computed in AQUASIM 2.0 (Reichert, 1998), was performed to evaluate the relative importance of parameters on the Monod model output. The parameters of interest were the kinetic and stoichiometric parameters, including X, C_{ini}, K_i, K_s, $Y_{x/s}$ and μ_{max}. A 1% change in a given model input parameter was applied, while the others were kept constant, and the effect of the change on the model was evaluated. From the plot, it is clear that minor adjustments in the parameters; K_i, K_s, $Y_{x/s}$ and μ_{max} are critical to the model output. The model sensitivity to the parameters K_i and μ_{max} increases from zero and reaches a maximum at 240 hours then decreases again to zero, exhibiting the behaviour of the absolute value of the sensitivity function (Reichert, 1998). On the other hand, the model sensitivity to the parameter $Y_{x/s}$, remained at zero until after 240 hours, after which it increased reaching a maximum at 312 hours. Relatively, the model was less sensitive to the parameter K_s, suggesting that this constant is of minor significance to reactor performance. The dependence of the biomass concentration (X) on the initial metal concentration (C_{ini}) is identifiable, as such is an important aspect that has to be taken into consideration for evaluating the performance of bioremediation bioreactors utilizing growing biomass.

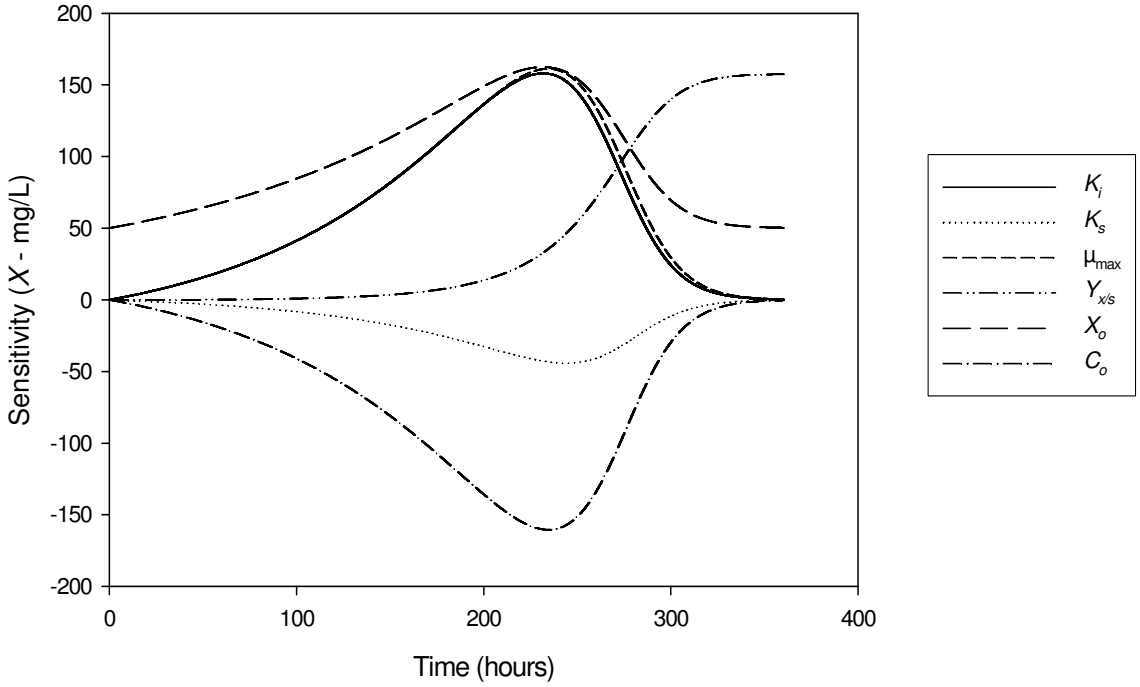

Figure 4.16: Time course of the sensitivity functions of SRB biomass concentration (*X*) at an initial metal concentration of 75 mg/L with respect to other kinetic parameters.

4.4 SUMMARY

In the original SRB consortium, microorganisms belonging to two genera; *Enterococcus* and *Staphylococcus* were detected. However, exposure to media containing Sr^{2+}, Co^{2+} and Cs^{+} led to the emergence of new bacterial strains; *Citrobacter, Stenotrophomonas* and *Paenibacillus* sp. The presence of Sr^{2+} in the growth medium resulted in the complete eradication of the original consortium members, and the emergence of *Citrobacter* sp. These microorganisms demonstrated a unique high Sr^{2+} tolerance, which permitted positive bacterial growth and metabolism, as well as high metal removal capacities in the presence of Sr^{2+} concentrations of up to 500 mg/L. However, there was an obvious dependence of bacterial activities (growth and sulphate reduction) on the initial Sr^{2+} concentration, where an increase in metal concentration corresponded to a decrease in bacterial activities. Likewise, Sr^{2+} removal from solution was

dependent on the bacterial concentration, as complete Sr^{2+} removal was observed where the toxic and inhibitory effects of the metal on the culture was low. This study is the first to demonstrate high Sr tolerance among the *Citrobacter* sp., and it can be assumed this trait is genetically intrinsic as the microorganisms were not pre-exposed to Sr. Results from this study also provide strong evidence *Paenibacillus* sp. and *Enterococcus* sp., isolated from the Co-contaminated SRB bioreactors are resilient towards Co^{2+} and facilitate its removal through biosorption and bioreduction. However, initial Co^{2+} concentration ≥300 mg/L had a detrimental effect on the growth and metabolism of the SRB consortium. As a result, the metabolism-dependent Co^{2+} removal (bioreduction) capacity of the cultures was also lowered. At such high concentration it can be assumed that biosorption processes supersede bioreduction. On the other hand, the presence of Cs^{+} resulted in the replacement of *Staphylococcus* sp. with *Stenotrophomonas* sp., while *Enterococcus* sp were retained. The bacterial isolates obtained from the Cs^{+}-contaminated sulphidogenic bioreactors displayed a high degree of Cs^{+} tolerance, as a prolonged exponential growth phase was observed.

Microbial Cs^{+} removal from solution occurred mainly through biosorption processes, and the removal capacity decreased with increasing initial concentration. Although Cs^{+} is a weak Lewis acid that exhibits a low tendency to form complexes with ligands, complete removal was observed at initial concentration ≤75 mg/L, suggesting that the present SRB consortium may possess extremely hydrophilic binding sites that promote the uptake of Cs^{+} onto bacterial cells. In summary, through experimental and model simulations, we have been able to demonstrate the interrelationships between SRB activities (growth, metabolism and diversity) and individual fission product cations removal from solution. Results obtained indicate that satisfactory (up to 100%) metal removal can be attained, where the toxic and inhibitory effects of the metal on the bacterial culture are minimal. Generally, the sensitivity of the original SRB culture towards the different metals was in the order Sr>Co≥Cs. It is evident that the biosorption mechanism and cell capability can also be influenced by chemical and physical properties of the target metal ion itself, thereby determining cell viability (Veglio and Beolchini, 1997). Therefore, elucidation of mechanisms active during bacterial metal sequestration is essential, in order to establish consistency, and for successful exploitation of the phenomenon in realistic settings of industrial wastewater treatment.